Vibrational Spectroscopic and Density Functional Studies on Intramolecular Hydrogen Bonding and CH···O Interaction

A Thesis Submitted to
the Graduate School of Science
Hiroshima University

Takanori Harada

Department of Chemistry, Graduate School of Science
Hiroshima University
Higashi-Hiroshima, Japan

2001

主　論　文

ACKNOWLEDGMENTS

CONTENTS

LIST OF PUBLICATIONS

Chapter 1

Infrared Spectroscopic Evidence for an Attractive Intramolecular 1,5-CH···O
Interaction in 1-Methoxy-2-(methylthio)ethane
Hiroshi Yoshida, Takanori Harada, Keiichi Ohno, and Hiroatsu Matsuura
Chem. Commun. **1997**, 2213–2214.

Chapter 2

Conformational Stabilization by Intramolecular OH···S and CH···O
Interactions in 2-(Methylthio)ethanol. Matrix-Isolation Infrared
Spectroscopy and ab Initio MO Calculations
Hiroshi Yoshida, Takanori Harada, Tomoko Murase, Keiichi Ohno, and
Hiroatsu Matsuura
J. Phys. Chem. A **1997**, *101*, 1731–1737.

Chapter 3

Conformational and Vibrational Analyses of 2-Methoxyethanol and
2-(Methylthio)ethanol by Density Functional Theory
Hiroshi Yoshida, Takanori Harada, and Hiroatsu Matsuura
J. Mol. Struct. **1997**, *413/414*, 217–226.

Chapter 4

Implications of Intramolecular OH···Se Hydrogen Bonding and CH···O
Interaction in the Conformational Stabilization of 2-(Methylseleno)ethanol
Studied by Vibrational Spectroscopy and Density Functional Theory
Takanori Harada, Hiroshi Yoshida, Keiichi Ohno, Hiroatsu Matsuura,
Jian Zhang, Michio Iwaoka, and Shuji Tomoda
J. Phys. Chem. A, in press.

General Introduction

Intramolecular and intermolecular interactions are, among others, the important factors that determine the molecular properties and functions. Hydrogen bonding, in particular, is of primary importance. A large number of studies of hydrogen bonding have in fact been performed on a variety of organic and biological compounds by using pertinent experimental and theoretical methods.[1,2] From the viewpoint of structural chemistry, hydrogen bonding plays an important role in the determination of the molecular structure.

The conformational analysis of molecules is important for elucidating a relation between intramolecular and intermolecular interactions and the conformational stabilization. Previously, the molecules containing the OCH_2CH_2OH group, which are the simplest models that form intramolecular hydrogen bonding, have been studied.[3-11] For example, 2-methoxyethanol, $CH_3OCH_2CH_2OH$, assumes only the trans–gauche$^{\pm}$–gauche$^{\mp}$ conformation in an argon matrix, as stabilized by intramolecular hydrogen bonding between the hydroxyl hydrogen atom and the ether oxygen atom.[10] It is well known that the sulfur atom can also participate in the formation of hydrogen bonding. The previous microwave spectroscopic studies have shown that the molecules of 2-mercaptoethanol, $HSCH_2CH_2OH$,[12] and 2-(methylthio)ethanol, $CH_3SCH_2CH_2OH$,[13] in the gas phase adopt the conformation which is stabilized by intramolecular OH⋯S hydrogen bonding. The selenium atom of the fourth periodic element has been generally recognized to have less ability to participate in hydrogen bonding than the oxygen and sulfur atoms. Actually, the existence of OH⋯Se hydrogen bonding has been found only in a few organic crystals.[14,15] In this work, the distinct existence of OH⋯Se hydrogen bonding in the isolated state is shown.

Contrary to the well-recognized hydrogen bonding mentioned above, much less attention has been paid to weaker interactions involving less electronegative elements such as carbon. This is primarily due to practical considerations; weaker interactions are harder to observe and measure experimentally and require more sophisticated theoretical techniques to obtain realistic results.[16] In recently years, however, many crystallographic studies have been performed on weaker interactions involving the C–H group.[15] The existence of CH⋯O

2

interactions was first confirmed in organic crystals[17,18] and was ensured crystallographically in many organic compounds.[19]

Although CH$\cdots$O interaction is weaker than typical hydrogen bonding such as OH$\cdots$O and NH$\cdots$O, this interaction is attractive and plays an important role in the conformational stabilization. In a previous study on 1,2-dimethoxyethane, $CH_3OCH_2CH_2OCH_3$, it was shown that the trans–gauche$^{\pm}$–gauche$^{\mp}$ conformer exists in an argon matrix and is stabilized by intramolecular CH$\cdots$O interaction between a hydrogen atom in the methyl group and the oxygen atom.[20] A later theoretical study has shown the importance of intramolecular CH$\cdots$O interaction in the conformational stabilization of this molecule.[21] The CH$\cdots$S interaction, on the other hand, has been found only in a few organic crystals,[19] but the property of this interaction has not been clarified yet. In this work, the relevance of CH$\cdots$O and CH$\cdots$S interactions to the conformational stabilization is studied.

The experimental studies of molecular interactions have been performed primarily by infrared and Raman spectroscopy, NMR, and crystal structure analysis. Among these experimental techniques, matrix-isolation infrared spectroscopy is especially useful for investigating relations between molecular conformations and intramolecular interactions in the isolated molecular state and is easily collaborated with theoretical calculations. In quantum chemical calculations on molecular systems with possible interactions involved, it is essential to take account of electron correlation. Density functional calculations, which have been rapidly developed in recent years, satisfy this requirement. In addition, a precise vibrational wavenumber scaling method, called a wavenumber-linear scaling (WLS) method, has been established, which predicts vibrational wavenumbers with high accuracy.[22] The present thesis work was performed by combining matrix-isolation infrared spectroscopy and density functional theory.

This thesis consists of four chapters. In Chapter 1, the properties of intramolecular CH$\cdots$O and CH$\cdots$S interactions in 1-methoxy-2-(methylthio)ethane, $CH_3OCH_2CH_2SCH_3$, are discussed. In this molecular system, both of the interactions are possible for conformational stabilization. In Chapters 2–4, matrix-isolation infrared spectroscopic and theoretical studies on

intramolecular hydrogen bonding in a series of $CH_3XCH_2CH_2OH$ compounds [ME (X = O), MTE (X = S), and MSE (X = Se)] are described. In Chapter 2, the conformational stabilization by intramolecular OH$\cdots$S and CH$\cdots$O interactions in MTE is studied and the conformational stability of MTE is compared with that of ME. The conformational and vibrational analyses on ME and MTE by density functional calculations are further discussed in Chapter 3. The conformational stabilization by intramolecular OH$\cdots$Se hydrogen bonding in MSE is studied in Chapter 4, where the conformational stabilization energies by intramolecular OH$\cdots$X hydrogen bonding (X = O, S, and Se) and a relation between the molecular geometry and intramolecular hydrogen-bonded O–H stretching wavenumber are discussed on the basis of the results of density functional calculations.

References

(1) Jeffrey, G. A.; Saenger, W. *Hydrogen Bonding in Biological Structures*; Springer: Berlin, 1994.

(2) Scheiner, S. *Hydrogen Bonding: A Theoretical Perspective*; Oxford University Press: New York, 1997.

(3) Frei, H.; Ha, T.-K.; Meyer, R.; Günthard, Hs. H. *Chem. Phys.* **1977**, *25*, 271–298.

(4) Takeuchi, H.; Tasumi, M. *Chem. Phys.* **1983**, *77*, 21–34.

(5) Park, G. G.; Tasumi, M. *J. Phys. Chem.* **1991**, *95*, 2757–2762.

(6) Iwamoto, R. *Spectrochim. Acta, Part A* **1971**, *27*, 2385–2399.

(7) Singelenberg, F. A. J.; van der Maas, J. H. *J. Mol. Struct.* **1991**, *243*, 111–122.

(8) Singelenberg, F. A. J.; Lutz, E. T. G.; van der Maas, J. H.; Jalsovszky, G. *J. Mol. Struct.* **1991**, *245*, 173–182.

(9) Singelenberg, F. A. J; van der Maas, J. H.; Kroon-Batenburg, L. M. J. *J. Mol. Struct.* **1991**, *245*, 183–194.

(10) Yoshida, H.; Takikawa, K.; Ohno, K.; Matsuura, H. *J. Mol. Struct.* **1993**, *299*, 141–147.

(11) Yoshida, H.; Takikawa, K.; Kaneko, I.; Matsuura, H. *J. Mol. Struct. (THEOCHEM)* **1994**, *311*, 205–210.

(12) Sung, E.-M.; Harmony, M. D. *J. Am. Chem. Soc.* **1977**, *99*, 5603–5608.

(13) Marstockk, K.-M.; Møllendal, H.; Uggerud, E. *Acta Chem. Scand.* **1989**, *43*, 26–31.

(14) Kivekäs, R.; Laitalainen, T. *Acta Chem. Scand.* **1983**, *B37*, 61–64.

(15) Desiraju, G. R.; Steiner, T. *The Weak Hydrogen Bond: In Structural Chemistry and Biology*; Oxford University Press: New York, 1999.

(16) Platts, J. A.; Howard, S. T.; Woźniak, K. *Chem. Commun.* **1996**, 63–64.

(17) Sutor, D. J. *Nature* **1962**, *195*, 68–69.

(18) Sutor, D. J. *J. Chem. Soc.* **1963**, 1105–1110.

(19) Taylor, R.; Kennard, O. *J. Am. Chem. Soc.* **1982**, *104*, 5063–5070.

(20) Yoshida, H.; Kaneko, I.; Matsuura, H.; Ogawa, Y.; Tasumi, M. *Chem.*

Phys. Lett. **1992**, *196*, 601–606.

(21)   Tsuzuki, S.; Uchimaru, T.; Tanabe, K.; Hirano, T. *J. Phys. Chem.* **1993**, *97*, 1346–1350.

(22)   Yoshida, H.; Ehara, A.; Matsuura, H. *Chem. Phys. Lett.* **2000**, *325*, 477–483.

Chapter 1

Matrix-Isolation Infrared Spectroscopic and Density Functional Studies on Intramolecular CH···O Interaction in 1-Methoxy-2-(methylthio)ethane

Abstract

Intramolecular interactions in 1-methoxy-2-(methylthio)ethane have been studied by matrix-isolation infrared spectroscopy and density functional theory. In an argon matrix, the conformer with trans–trans–gauche$^{\pm}$ (TTG) around the $CH_3O-CH_2-CH_2-SCH_3$ bonds is the most stable and the conformer with trans–gauche$^{\pm}$–gauche$^{\mp}$ (TGG′) is the second most stable. The energy difference between these two conformers was estimated to be 0.69 ± 0.10 kJ mol^{-1}. The high stability of the TGG′ conformer is due to intramolecular 1,5-CH$\cdots$O interaction. The G′GT conformer, in which intramolecular 1,5-CH$\cdots$S interaction would be expected, is the least stable. These results show that 1,5-CH$\cdots$O interaction stabilizes the relevant conformations of 1-methoxy-2-(methylthio)ethane, while 1,5-CH$\cdots$S interaction is not strong enough to stabilize the conformation of this molecule. The length of the (S)C–H bond associated with 1,5-CH$\cdots$O interaction is shorter than the lengths of other (S)C–H bonds by about 0.003 Å.

1.1 Introduction

Intramolecular and intermolecular interactions are important for determining the structures of organic and biological molecules.[1] Besides typical hydrogen bonding such as OH···O and NH···O, weak interactions, in which C–H group is involved, have been found in many organic crystals.[2-4] Recent studies on isolated molecules have shown that intramolecular CH···O interactions play an important role in the conformational stabilization of molecules. One of the initial studies on this interaction showed that the conformational stabilities of 1,2-dimethoxyethane (DME), $CH_3OCH_2CH_2OCH_3$, in an argon matrix are governed primarily by intramolecular 1,5-CH···O interaction.[5] Since this work was reported, a considerable number of theoretical studies have been published, which dealt with the conformational properties of this molecule by paying special attention to this peculiar interaction.[6-10] These theoretical studies have shown the importance of this interaction in the conformational stabilization of the DME molecule, in agreement with the experimental results by gas-phase electron diffraction[11] and matrix-isolation and gas-phase infrared spectroscopy.[5,12]

1-Methoxy-2-(methylthio)ethane (MMTE), $CH_3OCH_2CH_2SCH_3$, which is an analogous compound of DME, is expected to assume molecular conformations that would be stabilized by intramolecular 1,5-CH···O and 1,5-CH···S interactions. In this work, the properties of these interactions and the molecular conformations of MMTE have been investigated by matrix-isolation infrared spectroscopy and density functional theory. To evaluate experimentally the energy difference between the relevant conformers, temperature-variable matrix-isolation infrared spectroscopy[13,14] was utilized.

1.2 Experimental Section

MMTE was synthesized by the following reaction.[15]

$$CH_3OCH_2CH_2Cl + CH_3SNa \text{ (aq)} \xrightarrow[\text{60 °C, 30 h}]{\text{NaOH}} CH_3OCH_2CH_2SCH_3 + NaCl$$
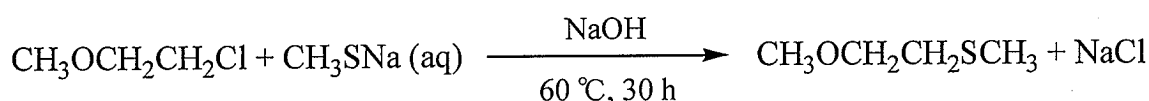
The product in the organic layer was purified by distillation and the purity was checked by gas chromatography to be better than 98%.

Matrix-isolation infrared spectra of MMTE were measured with a JEOL JIR-40X Fourier transform spectrophotometer equipped with a TGS detector. Premixed gas of Ar/MMTE = 2000 was slowly sprayed onto a cesium iodide plate cooled to 11 K by an Iwatani CryoMini D105 refrigerator. The spectra were obtained by coaddition of 100 scans at a resolution of 1 cm^{-1}. To study the spectral changes with increasing temperature, the deposited sample was annealed at different temperatures up to 41 K.

The temperature-variable matrix-isolation infrared spectra of MMTE were measured by depositing the premixed gas (Ar/MMTE = 1000) at several temperatures ranging from 298 K to 473 K onto a cesium iodide plate kept at 11 K by the same refrigerator as mentioned above. By using this method, the populations of the deposited sample frozen at 11 K can be assumed to be the same as the populations at the temperature of the gas sample immediately before the deposition.[13,14] The spectra were recorded on a JASCO FT/IR-350 spectrometer equipped with a DTGS detector by coaddition of 100 scans at a resolution of 1 cm^{-1}.

1.3 Calculations

Density functional calculations of the energies, structural parameters, and vibrational wavenumbers for 12 optimized conformers, shown in Figure 1.1, of MMTE were performed by using Becke's three-parameter hybrid functional[16] combined with the Lee–Yang–Parr correlation functional[17] (B3LYP). The density functional calculations were carried out with the Gaussian 98 program.[18] The vibrational wavenumbers calculated by the B3LYP/6-311+G** method were scaled by the wavenumber-linear scaling (WLS) method.[19]
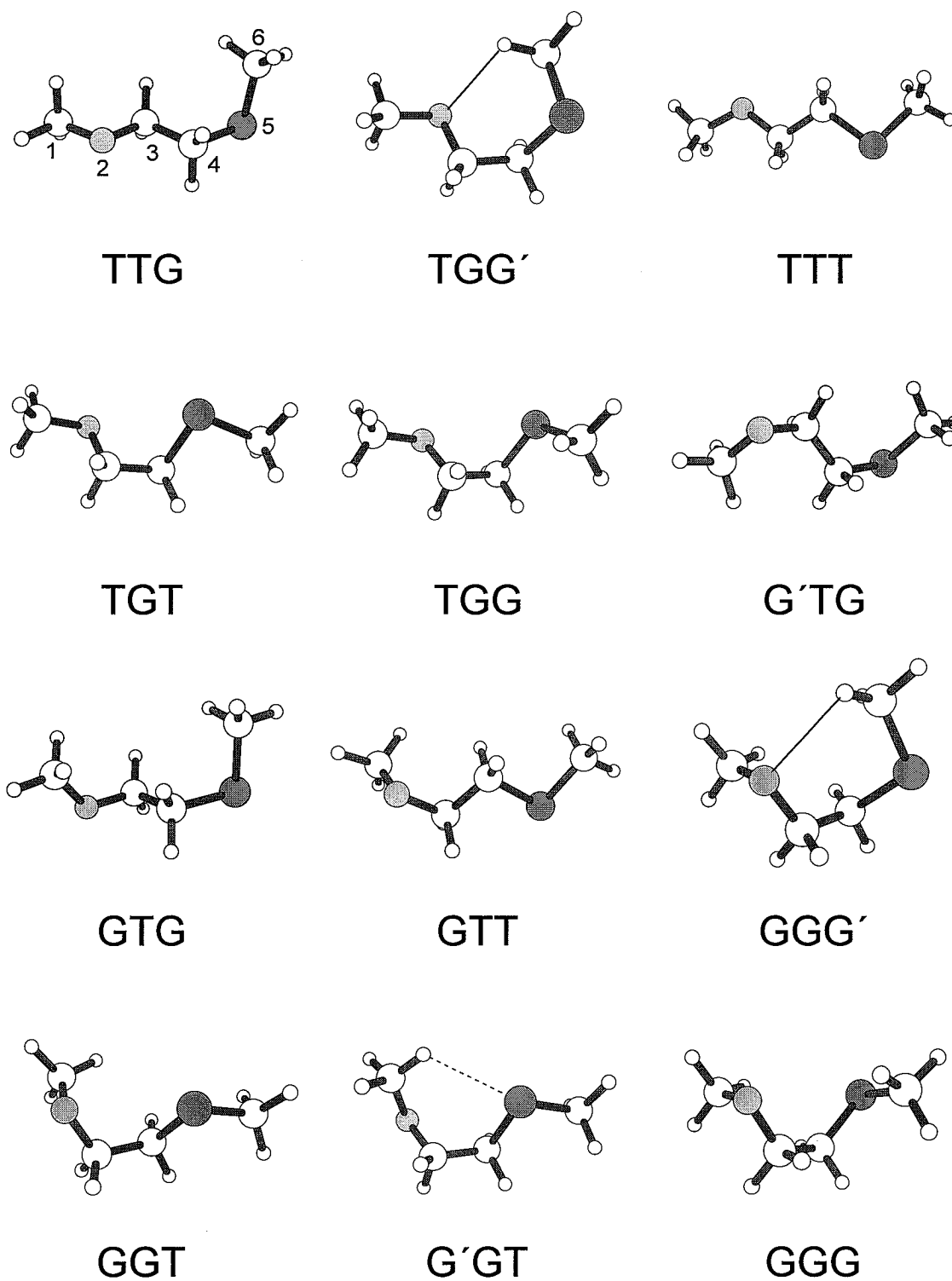
Figure 1.1 Optimized structures of 12 conformers of 1-methoxy-2-(methylthio)ethane. The solid lines indicate intramolecular 1,5-CH···O interaction, and the dashed line indicates intramolecular 1,5-CH···S interaction. Minimum-energy geometries for the G′GG and G′GG′ conformers were not attained.

Table 1.1 Relative Energies Corrected for Zero-Point Energies of the Conformers of 1-Methoxy-2-(methylthio)ethane Calculated by the B3LYP/6-311+G(2d,p) Method

conformer	energy/kJ mol^{-1} [a]	conformer	energy/kJ mol^{-1} [a]
TTG	0.000	GTT	8.241
TGG′ [b]	0.557	GGG′ [b]	8.774
TTT	2.221	GGT	10.027
TGT	4.487	G′GT [c]	11.618
TGG	4.576	GGG	11.655
G′TG	5.582	G′GG [c]	–[d]
GTG	6.346	G′GG′ [b,c]	–[d]

[a] Relative energies with respect to the energy of the TGG′ conformer. [b] 1,5-CH⋯O interaction is involved. [c] 1,5-CH⋯S interaction would be possible. [d] Minimum-energy geometry was not attained.

1.4 Results and Discussion

1.4.1 Energies of Conformers

The molecular conformation of MMTE is designated for a sequence of the three bonds CH$_3$O–CH$_2$–CH$_2$–SCH$_3$ by the symbols T for trans, G for gauche^{+}, and G′ for gauche$^{\mp}$. The relative energies corrected for zero-point energies of 12 optimized conformers of MMTE calculated by the B3LYP/6-311+G(2d,p) method are given in Table 1.1, where the intramolecular interactions involved are indicated for the relevant conformers.

The calculated results indicate that the TGG′ conformer, which is stabilized by 1,5-CH⋯O interaction like the corresponding conformer of DME,[5-12] and the TTG conformer have almost the same conformational stabilities. The G′GT conformer, in which 1,5-CH⋯S interaction would be expected, is, however, the second least stable among those optimized in the calculations. The lability of

this conformer is caused primarily by the unstable conformation of gauche around the CO–CC bond and of trans around the CS–CC bond. It is suggested therefore that 1,5-CH⋯S interaction is not strong enough to stabilize the G'GT conformer by compensating the conformational unstabilities of the CO–CC and CS–CC bonds. These results show that 1,5-CH⋯O interaction stabilizes the relevant conformations of MMTE, while 1,5-CH⋯S interaction does not work in effect for stabilizing the conformation of MMTE.

1.4.2 Matrix-Isolation Infrared Spectra and Molecular Conformation

The matrix-isolation infrared spectra in the 600–1500 cm^{-1} region of MMTE annealed at different temperatures are shown in Figure 1.2, where the calculated spectra of the most stable two conformers, TTG and TGG', are also shown. The wavenumbers calculated at the B3LYP/6-311+G** level were scaled by the WLS method,[19] which has been shown to give an excellent agreement with the experimental wavenumbers.

The normal coordinate analysis shows that the three conformers, TTG, TGG', and TTT, exist in an argon matrix at 11 K. The observed and calculated wavenumbers and the vibrational assignments for the TTG and TGG' conformers are given in Tables 1.2 and 1.3, respectively. A distinct band assigned to the TTT conformer is observed at 1131 cm^{-1}.

On annealing the matrix sample at 29 K, the bands due to the TGG' conformer, such as those at 1016, 1127, and 1176 cm^{-1}, and the bands due to the TTT conformer decrease in intensity. At 38 K, the TTG conformer dominantly exists in an argon matrix. Since the annealing process induces a transformation of less stable conformers trapped in a matrix into the most stable conformer, the TTG conformer is shown to be the most stable in an argon matrix.

1.4.3 Energy Difference between the TTG, TGG', and TTT Conformers

The infrared spectra in an argon matrix measured with changing sample temperature are shown in Figure 1.3. The changes of the relative intensities of the

13
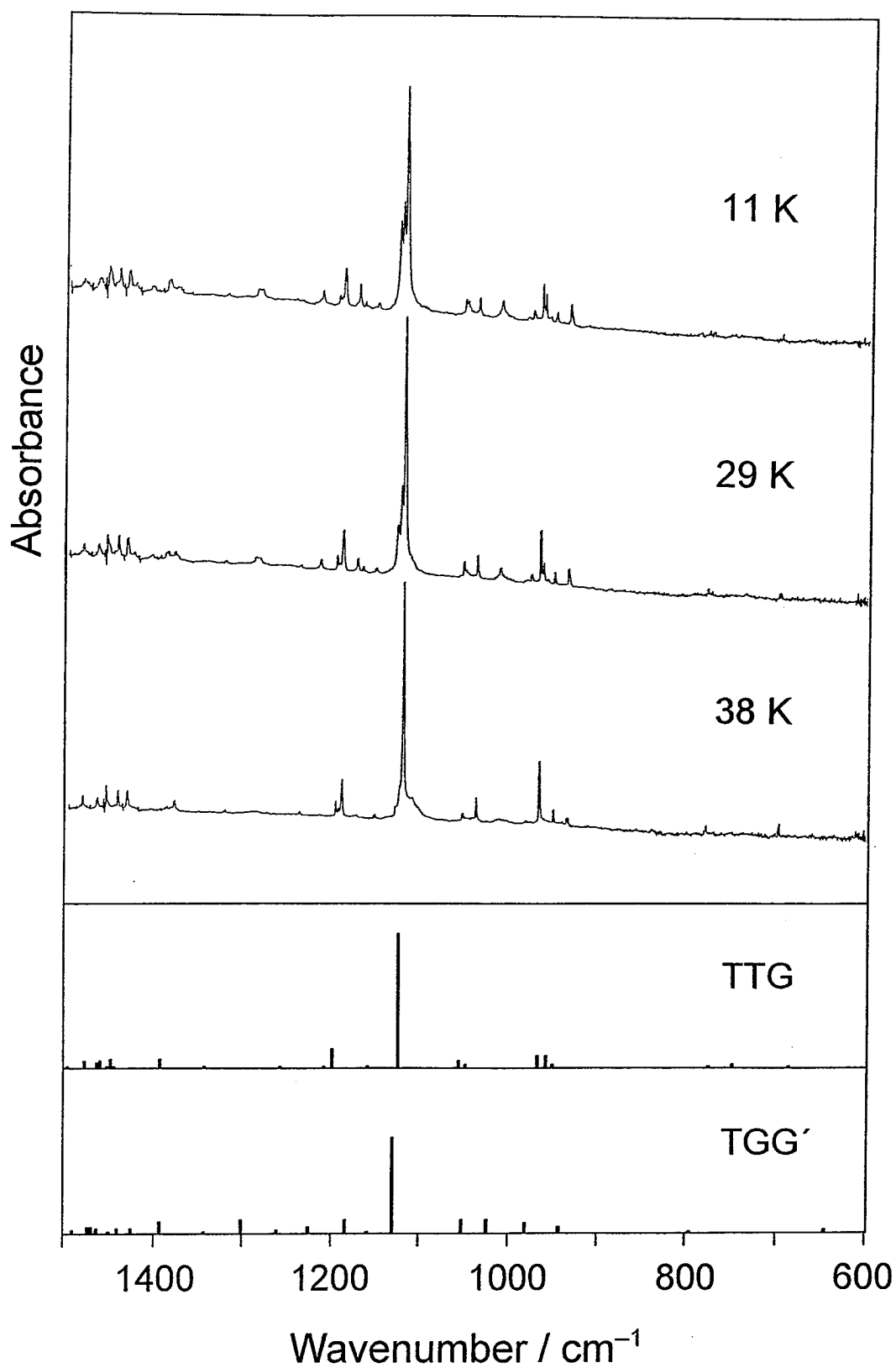
Figure 1.2 Infrared spectra in the 600–1500 cm⁻¹ region of 1-methoxy-2-(methylthio)ethane in an argon matrix annealed at 11, 29, and 38 K, and the calculated spectra of the TTG and TGG′ conformers.

Table 1.3 Observed and Calculated Wavenumbers in the 600–1500 cm^{-1} Region and Vibrational Assignments for the TTG Conformer of 1-Methoxy-2-(methylthio)ethane

$v_{obs}{}^a$/cm^{-1}	$v_{calc}{}^b$/cm^{-1}	vibrational assignment^c
	1497	C_aH_2 scissor (78), CH_3O ip-asym deform (10), CH_3O sym deform (8)
	1478	CH_3O ip-asym deform (75), C_aH_2 scissor (17)
1481 vw	1463	CH_3O op-asym deform (95)
1465 vw	1461	CH_3S ip-asym deform (88)
1455 w	1453	CH_3O sym deform (71), C_bH_2 scissor (10)
1442 w	1448	C_bH_2 scissor (58), CH_3S op-asym deform (31), CH_3O sym deform (8)
1431 w	1444	CH_3S op-asym deform (59), C_bH_2 scissor (25), CH_3O sym deform (7)
1380 vw	1393	C_aH_2 wag (85)
1323 vw	1345	CH_3S sym deform (104)
	1293	C_aH_2 twist (56), C_bH_2 twist (25)
1240 vw	1259	C_bH_2 wag (86)
1200 vw	1210	C_bH_2 twist (34), C_aH_2 twist (28), C_aH_2 rock (23)
1192 w	1199	CH_3O ip-rock (64), C–O stretch (11), C_aH_2 wag (9)
1156 vw	1159	CH_3O op-rock (86)
1123 s	1126	CH_3–O stretch (67), C–O stretch (33)
1057 w	1058	C_aH_2 rock (25), C_bH_2 rock (17), CH_3S ip-rock (17)
1042 w	1049	C–C stretch (63)
971 w	968	CH_3S op-rock (53), C–O stretch (16), CH_3–O stretch (11)
954 vw	959	C–O stretch (38), CH_3S op-rock (31), CH_3–O stretch (21)
939 w	950	CH_3S ip-rock (54), C_bH_2 twist (17), C_aH_2 rock (15)
784 vw	775	C_bH_2 rock (58), C_aH_2 rock (25), C–S stretch (10)
	749	C–S stretch (61), CH_3–S stretch (17), C_bH_2 rock (10)
702 vw	687	CH_3–S stretch (89), C–S stretch (10)

^{a} Observed wavenumbers for an argon matrix. Approximate relative intensities: s, strong; m, medium; w, weak; vw, very weak. ^{b} Calculated by the B3LYP/6-311+G** method and scaled by the WLS method.[19] ^{c} Vibrational assignment for $CH_3OC_aH_2C_bH_2SCH_3$ is given in terms of the group coordinates. Key: sym, symmetric; asym, asymmetric; ip, in-plane; op, out-of-plane. Potential energy distributions (%) evaluated from the B3LYP/6-311+G** calculations are shown in parentheses.

Table 1.4 Observed and Calculated Wavenumbers in the 600–1500 cm^{-1} Region and Vibrational Assignments for the TGG′ Conformer of 1-Methoxy-2-(methylthio)ethane

$\nu_{obs}{}^{b}$/cm^{-1}	$\nu_{calc}{}^{c}$/cm^{-1}	vibrational assignment^{d}
	1491	C_aH_2 scissor (47), CH_3O ip-asym deform (30), CH_3O sym deform (14)
	1474	CH_3O ip-asym deform (59), C_aH_2 scissor (39)
	1469	CH_3S ip-asym deform (92)
	1463	CH_3O op-asym deform (94)
	1451	CH_3O sym deform (80), C_aH_2 scissor (13)
	1442	CH_3S op-asym deform (89)
1426 vw	1425	C_bH_2 scissor (98)
1389 vw	1394	C_aH_2 wag (87)
	1344	CH_3S sym deform (97)
1289 vw	1303	C_bH_2 wag (57), C_aH_2 twist (30), CH_3S sym deform (9)
1249 vw	1262	C_bH_2 twist (29), C_aH_2 twist (21), C_bH_2 wag (20)
1218 vw	1226	C_aH_2 twist (33), C_bH_2 twist (17), CH_3O ip-rock (14)
1176 w	1184	CH_3O ip-rock (50), C_bH_2 twist (26), C–O stretch (5)
	1160	CH_3O op-rock (86)
1127 m	1132	CH_3–O stretch (58), C–O stretch (33), C–C stretch (9)
1055 w	1054	C_aH_2 rock (27), C–C stretch (26), C_bH_2 rock (10)
1016 w	1024	CH_3S ip-rock (27), CH_3–O stretch (19), C–O stretch (13)
980 vw	982	CH_3S op-rock (28), C_aH_2 rock (25), C–C stretch (15)
967 w	973	CH_3S op-rock (65), C_aH_2 rock (16)
939 w	943	CH_3S ip-rock (33), C–O stretch (22), O–C–C bend (12)
	797	C_bH_2 rock (59), C–O stretch (22), CH_3–O stretch (8)
	708	CH_3–S stretch (86), C–S stretch (19)
	647	C–S stretch (74), CH_3–S stretch (20), C–C–S bend (10)

$^{a-c}$ See footnotes a–c, respectively, of Table 1.3.

16
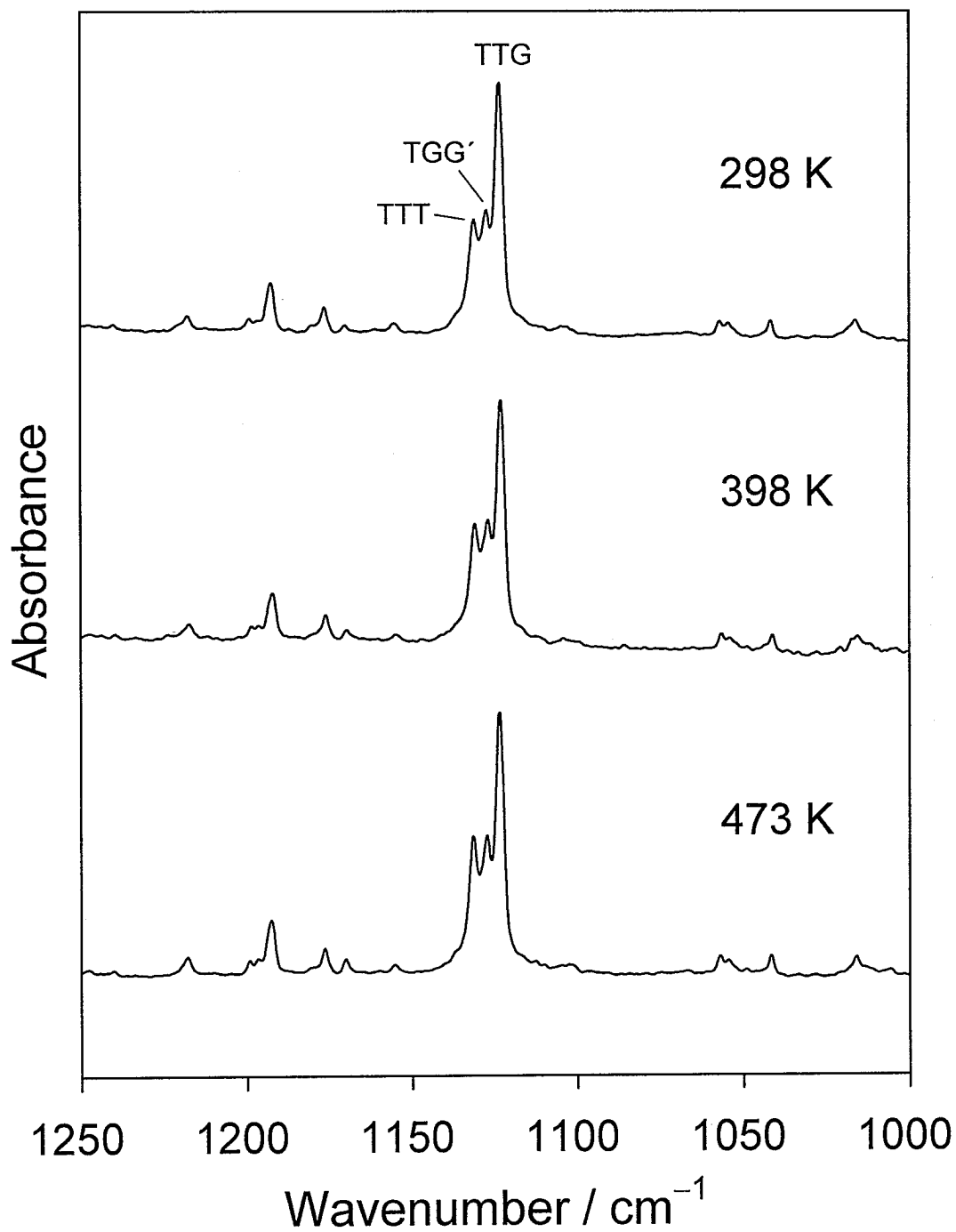
Figure 1.3   Infrared spectra of 1-methoxy-2-(methylthio)ethane in an argon matrix with changing sample temperature at 298 K, 398 K, and 473 K. The sample was deposited at 11 K.
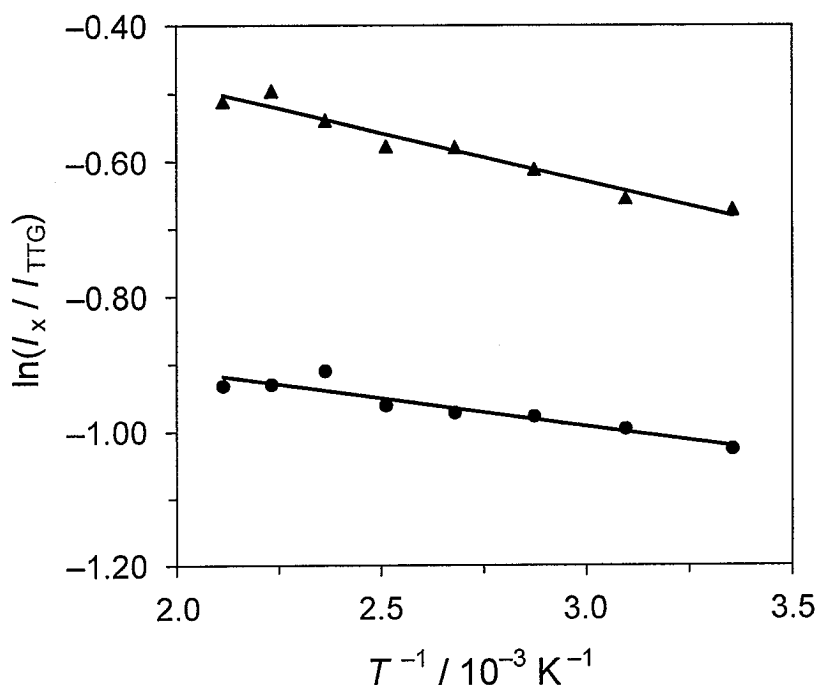
Figure 1.4 Logarithmic intensity ratio $\ln(I_x/I_{TTG})$ [● : x = TGG′, ▲ : x = TTT] of
1-methoxy-2-(methylthio)ethane as a function of reciprocal temperature.

bands due to the TTG conformer (1123 cm^{-1}), the TGG′ conformer (1127 cm^{-1}), and the TTT conformer (1131 cm^{-1}) are very small when the temperature is changed. This spectral observation suggests that the energy differences between the TTG and TGG′ conformers and between the TTG and TTT conformers are small. To evaluate the energy differences between these three conformers more precisely, the temperature dependence of the intensity ratio of the bands are plotted in Figure 1.4, where the area intensities of the bands of each conformer are evaluated by analyzing the spectral profiles in the region of 1100–1150 cm^{-1} by fitting with Lorentzian components. This analysis shows that the TTG conformer is more stable than the TGG′ conformer by 0.69±0.10 kJ mol^{-1} and is more stable than the TTT conformer by 1.20±0.10 kJ mol^{-1}. These results agree with the conformational stabilities deduced from the annealing effect of the matrix sample. The high stability of the TGG′ conformer in the isolated state is thus experimentally evidenced.

The present experimental energy differences between the relevant three conformers are compared with the theoretical results by B3LYP/6-311+G(2d,p), as summarized in Table 1.1. The energy difference, calculated by the B3LYP/6-311+G(2d,p) method, between the TGG′ and TTG conformers is 0.56 kJ mol^{-1} and that between the TTT and TTG conformers is 2.22 kJ mol^{-1}. The conformational energy differences calculated by this method are consistent with the experimental results of matrix-isolation infrared spectroscopy.

1.4.4 Molecular Geometries of the TTG and TGG′ Conformers

The bond lengths, bond angles, and torsion angles calculated by the B3LYP/6-311+G(2d,p) method and the experimental structural parameters[20] for the TTG conformer of MMTE in crystals are given in Table 1.4. The calculated structural parameters of the TTG conformer are in good agreement with the experimental values.

To clarify the geometrical properties relevant to 1,5-CH···O interaction, the structural parameters for the TGG′ conformer calculated by the B3LYP/6-311+G(2d,p) method are compared with those for the TGG conformer, which has the conformational analogy to the TGG′ conformer but does not involve 1,5-CH···O interaction. These structural parameters are given in Table 1.5. The important structural difference between the two conformers is that the length of one of the three C_6–H bonds in the TGG′ conformer (1.0866 Å) is shorter than that of the corresponding bond in the TGG conformer (1.0897 Å) by 0.003 Å. This bond length is also shorter than the lengths of other C_6–H bonds in the TGG′ conformer by 0.003 Å. This particular C–H bond in the TGG′ conformer is made shorter in consequence of being involved in 1,5-CH···O interaction. This shortening of the bond length is a characteristic geometrical feature of CH···O interaction,[21-23] and the mechanism of the C–H bond contraction has been theoretically studied.[23-27] It was shown that the contraction originates from the redistribution of electron density in the C–H bond, induced when the bond comes close to a proton acceptor.[27] For the TGG′ conformer, the nonbonded interatomic CH···O distance is calculated to be 2.55 Å (Table 1.5), which is

19

Table 1.4 Structural Parameters of the TTG Conformer

structural parameters[a]	calculated[b]	experimental[c]
	Bond Lengths/Å	
C_1–H	1.0978	
	1.0980	
	1.0894	
C_1–O_2	1.4140	1.419
O_2–C_3	1.4188	1.4194
C_3–C_4	1.5194	1.508
C_4–S_5	1.8282	1.8031
S_5–C_6	1.8258	1.8028
C_6–H	1.0892	
	1.0897	
	1.0904	
	Bond Angles/deg	
C_1–O_2–C_3	112.86	111.60
O_2–C_3–C_4	108.00	108.10
C_3–C_4–S_5	113.64	113.13
C_4–S_5–C_6	101.28	99.78
	Torsion Angles/deg	
C_1–O_2–C_3–C_4	179.48	−178.06
O_2–C_3–C_4–S_5	−179.88	178.07
C_3–C_4–S_5–C_6	−78.75	−78.55

[a] For numbering of atoms, see Figure 1.1. [b] Calculated at the B3LYP/6-311+G(2d,p) level. [c] Crystal structures analyzed by X-ray diffraction.[21]

Table 1.5 Structural Parameters of the TGG′ and TGG Conformers

structural parameters[a]	TGG′	TGG
	Bond Lengths/Å	
C_1–H	1.0975	1.0978
	1.0980	1.0984
	1.0894	1.0892
C_1–O_2	1.4141	1.4126
O_2–C_3	1.4170	1.4125
C_3–C_4	1.5171	1.5182
C_4–S_5	1.8312	1.8326
S_5–C_6	1.8264	1.8242
C_6–H	1.0866[b]	1.0897
	1.0900	1.0901
	1.0904	1.0909
	Bond Angles/deg	
C_1–O_2–C_3	112.68	113.05
O_2–C_3–C_4	109.96	109.15
C_3–C_4–S_5	116.03	115.55
C_4–S_5–C_6	101.93	100.38
	Torsion Angles/deg	
C_1–O_2–C_3–C_4	–179.76	–175.85
O_2–C_3–C_4–S_5	70.22	71.87
C_3–C_4–S_5–C_6	–80.36	80.42
	Nonbonded Interatomic Distance/Å	
C_6H$\cdots$$O_2$	2.5478	

[a] For numbering of atoms, see Figure 1.1. Calculated at the B3LYP/6-311+G(2d,p) level. [b] C–H bond associated with 1,5-CH$\cdots$O interaction.

21

significantly shorter than the expected van der Waals separation of 2.70 Å. These results show that 1,5-CH⋯O interaction is attractive and is a dominant factor of stabilizing the TGG′ conformer.

1.5 Conclusions

Matrix-isolation infrared spectroscopy and density functional theory have clarified that the TGG′ conformer of MMTE has high conformational stability. Although the most stable conformer is TTG and the second most stable conformer is TGG′ in an argon matrix, the energy difference between the two conformers is only 0.69 ± 0.10 kJ mol^{-1}. This result shows that 1,5-CH⋯O interaction stabilizes the conformation of MMTE. The G′GT conformer, in which 1,5-CH⋯S interaction would be expected, is the least stable, indicating that 1,5-CH⋯S interaction is not strong enough to stabilize the conformation of MMTE. The length of the (S)C–H bond associated with 1,5-CH⋯O interaction is shorter than the lengths of other (S)C–H bonds by about 0.003 Å. The present study has shown the importance of intramolecular interactions in the conformational stabilization of MMTE.

References

(1) Jeffrey, G. A.; Saenger, W. *Hydrogen Bonding in Biological Structures*; Springer: Berlin, 1994.

(2) Sutor, D. J. *Nature* **1962**, *195*, 68–69.

(3) Sutor, D. J. *J. Chem. Soc.* **1963**, 1105–1110.

(4) Taylor, R.; Kennard, O. *J. Am. Chem. Soc.* **1982**, *104*, 5063–5070.

(5) Yoshida, H.; Kaneko, I.; Matsuura, H.; Ogawa, Y.; Tasumi, M. *Chem. Phys. Lett.* **1992**, *196*, 601–606.

(6) Tsuzuki, S.; Uchimaru, T.; Tanabe, K.; Hirano, T. *J. Phys. Chem.* **1993**, *97*, 1346–1350.

(7) Jaffe, R. L.; Smith, G. D.; Yoon, D. Y. *J. Phys. Chem.* **1993**, *97*, 12745–12751; Smith, G. D.; Jaffe, R. L.; Yoon, D. Y. *J. Phys. Chem.* **1993**, *97*, 12752–12759; Smith, G. D.; Jaffe, R. L.; Yoon, D. Y. *J. Am. Chem. Soc.* **1995**, *117*, 530–531.

(8) Müller-Plathe, F.; van Gunsteren, W. F. *Macromolecules* **1994**, *27*, 6040–6045; Liu, H.; Müller-Plathe, F.; van Gunsteren, W. F. *J. Chem. Phys.* **1995**, *102*, 1722–1730.

(9) Engkvist, O.; Åstrand P.-O.; Karlström, G. *J. Phys. Chem.* **1996**, *100*, 6950–6957.

(10) Williams, D. J.; Hall, K. B. *J. Phys. Chem.* **1996**, *100*, 8224–8229.

(11) Astrup, E. E. *Acta Chem. Scand., Ser. A* **1979**, *33*, 655–664.

(12) Yoshida, H.; Tanaka, T.; Matsuura, H. *Chem. Lett.* **1996**, 637–638.

(13) Felder, P.; Günthard, Hs. H. *Spectrochim. Acta, Part A* **1980**, *36*, 223–224.

(14) Kudoh, S.; Takayanagi, M.; Nakata, M. *Chem. Phys. Lett.* **1998**, *296*, 329–334.

(15) Ogawa, Y.; Ohta, M.; Sakakibara, M.; Matsuura, H.; Harada, I.; Shimanouchi, T. *Bull. Chem. Soc. Jpn.* **1977**, *50*, 650–660.

(16) Becke, A. D. *J. Chem. Phys.* **1993**, *98*, 5648–5652.

(17) Lee, C.; Yang, W.; Parr, R. G. *Phys. Rev. B* **1988**, *37*, 785–789.

(18) Frisch, M. J.; Trucks, G. W.; Schlegel, H. B.; Scuseria, G. E.; Robb, M.

A.; Cheeseman, J. R.; Zakrzewski, V. G.; Montgomery, J. A., Jr.; Stratmann, R. E.; Burant, J. C.; Dapprich, S.; Millam, J. M.; Daniels, A. D.; Kudin, K. N.; Strain, M. C.; Farkas, O.; Tomasi, J.; Barone, V.; Cossi, M.; Cammi, R.; Mennucci, B.; Pomelli, C.; Adamo, C.; Clifford, S.; Ochterski, J.; Petersson, G. A.; Ayala, P. Y.; Cui, Q.; Morokuma, K.; Malick, D. K.; Rabuck, A. D.; Raghavachari, K.; Foresman, J. B.; Cioslowski, J.; Ortiz, J. V.; Stefanov, B. B.; Liu, G.; Liashenko, A.; Piskorz, P.; Komaromi, I.; Gomperts, R.; Martin, R. L.; Fox, D. J.; Keith, T.; Al-Laham, M. A.; Peng, C. Y.; Nanayakkara, A.; Gonzalez, C.; Challacombe, M.; Gill, P. M. W.; Johnson, B.; Chen, W.; Wong, M. W.; Andres, J. L.; Gonzalez, C.; Head-Gordon, M.; Replogle, E. S.; Pople, J. A. *Gaussian 98*, revision A.5; Gaussian, Inc.: Pittsburgh, PA, 1998.

(19) Yoshida, H.; Ehara, A.; Matsuura, H. *Chem. Phys. Lett.* **2000**, *325*, 477–483.

(20) Yokoyama, Y.; Ohashi, Y. *Bull. Chem. Soc. Jpn.* **1998**, *71*, 1565–1571.

(21) Chapter 2 of this thesis. Yoshida, H.; Harada, T.; Murase, T.; Ohno, K.; Matsuura, H. *J. Phys. Chem. A* **1997**, *101*, 1731–1737.

(22) Hobza, P.; Havlas, Z. *Chem. Phys. Lett.* **1999**, *303*, 447–452.

(23) Gu, Y.; Kar, T.; Scheiner, S. *J. Am. Chem. Soc.* **1999**, *121*, 9411–9422.

(24) Caminati, W.; Melandri, S.; Moreschini, P.; Favero, P. G. *Angew. Chem. Int. Ed.* **1999**, *38*, 2924–2925.

(25) Hobza, P.; Špirko, V.; Selzle, H. L.; Schlag, E. W. *J. Phys. Chem. A* **1998**, *102*, 2501–2504.

(26) Hobza, P.; Špirko, V.; Havlas, Z.; Buchhold, K.; Reimann, B.; Barth, H.-D.; Brutschy, B. *Chem. Phys. Lett.* **1999**, *299*, 180–186.

(27) Cubero, E.; Orozco, M.; Hobza, P.; Luque, F. J. *J. Phys. Chem. A* **1999**, *103*, 6394–6401.

Chapter 2

Matrix-Isolation Infrared Spectroscopic Studies
on Conformation of 2-(Methylthio)ethanol

Abstract

The conformational stability of 2-(methylthio)ethanol has been studied by matrix-isolation infrared spectroscopy supplemented by ab initio molecular orbital calculations. In an argon matrix, the conformer with gauche$^{\pm}$–gauche$^{\pm}$–gauche$^{\mp}$ (GGg′) around the CS–C–C–OH bonds is the most stable and the G′Gg′ conformer is the second most stable. These and the TGg′ conformers are stabilized by intramolecular hydrogen bonding between the hydroxyl hydrogen atom and the sulfur atom. The relative strength of hydrogen bonding in these conformers is in order of GGg′ > TGg′ > G′Gg′ as estimated from the nonbonded OH$\cdots$S distance. In the G′Gg′ conformer, an additional intramolecular interaction between the methyl hydrogen atom and the hydroxyl oxygen atom is involved. The relative strength of this 1,5-CH$\cdots$O interaction in the G′Gg′ conformer is the least among the three relevant conformers with the G′G conformation around the CS–C–COH bonds. The calculated results indicate that the geometry of this conformational form is considerably distorted so that it is simultaneously accessible to both of the interactions. This geometry is, however, not best suited for the respective interactions to be the most effective. The results for 2-(methylthio)ethanol have been compared with those for 2-methoxyethanol, in which analogous intramolecular interactions are involved. This study emphasizes the importance of intramolecular interactions in the conformational stabilization of 2-(methylthio)ethanol and other relevant compounds.

2.1 Introduction

The conformation of molecules is determined by a number of factors including intramolecular and intermolecular interactions. One of those interactions responsible for the conformational stabilization is intramolecular hydrogen bonding. In order to elucidate the implications of intramolecular hydrogen bonding in the molecular conformation, many studies have been performed by vibrational spectroscopy on various relevant compounds, especially on those containing the OCH_2CH_2OH group.[1-9] For 1,2-ethanediol (ethylene glycol), $HOCH_2CH_2OH$, and 2-methoxyethanol (ME), $CH_3OCH_2CH_2OH$, the stable and less stable conformers have been identified by matrix-isolation infrared spectroscopy.[1-3,8] In an argon matrix at 11 K, the molecules of ME assume only the trans–gauche$^{\pm}$–gauche$^{\mp}$ conformation, which is stabilized by intramolecular hydrogen bonding between the hydroxyl hydrogen atom and the ether oxygen atom.[8]

The conformation of the molecules in which intramolecular hydrogen bonding is formed between a hydroxyl hydrogen atom and a sulfur atom has been studied for several compounds that contain the SCH_2CH_2OH group. The previous microwave spectroscopic studies have shown that the molecules of 2-mercaptoethanol, $HSCH_2CH_2OH$,[10] and 2-(methylthio)ethanol (MTE), $CH_3SCH_2CH_2OH$,[11] in the gas phase adopt the conformation which is stabilized by intramolecular OH···S hydrogen bonding. In a previous theoretical study,[12] ab initio molecular orbital (MO) calculations have been performed on several conformers of $CH_3XCH_2CH_2YH$ molecules, where X and Y are O or S, and the effect of the oxygen-by-sulfur substitution on the conformational stability and the relative strength of intramolecular YH···X hydrogen bonding have been discussed. There have been no close experimental studies, however, of the molecular conformation of MTE for understanding the effect of intramolecular OH···S hydrogen bonding on the conformation. In the molecule of MTE, another intramolecular interaction between one of the methyl hydrogen atoms and the hydroxyl oxygen atom, as mentioned below, may also be an important factor of the conformational stabilization.

27

Recent experimental[13,14] and theoretical[15] studies on 1,2-dimethoxyethane, $CH_3OCH_2CH_2OCH_3$, have shown that an intramolecular interaction between a hydrogen atom in the methyl group and the nonbonded oxygen atom plays an important role in determining the molecular conformation. This new type of interaction, termed 1,5-CH$\cdots$O interaction, is anticipated to be relevant also to MTE. Thus, two types of intramolecular interactions, OH$\cdots$S hydrogen bonding and 1,5-CH$\cdots$O interaction, are involved in the conformational stabilization of the MTE molecule, and their cooperative effect may give rise to high stability of particular conformations.

For the purpose of gaining experimental evidence for the implications of these intramolecular interactions in the conformational stabilization, the molecular conformation of MTE has been investigated by matrix-isolation infrared spectroscopy, supplemented by infrared and Raman spectroscopy in the condensed phases and by ab initio MO calculations on all possible conformers of this compound. The results are discussed in comparison with the conformational stability of ME studied by matrix-isolation infrared spectroscopy and ab initio MO calculations.[8]

2.2 Experimental Section

MTE was commercially supplied by Sigma Chemical Co. The infrared spectra of MTE in an argon matrix were measured with a JEOL JIR-40X Fourier transform spectrophotometer equipped with a TGS detector. Premixed gas of Ar/MTE = 4000 was slowly sprayed onto a cesium iodide plate cooled to 11 K by an Iwatani CryoMini D105 refrigerator. The spectra were obtained by coaddition of 100 scans at a resolution of 1 cm^{-1}. To study the spectral changes with increasing temperature, the deposited sample was annealed at different temperatures up to 41 K. The glassy state was obtained by spraying only the MTE gas onto a cesium iodide plate at 11 K. The infrared spectra of liquid MTE were measured at room temperature with a Nicolet Impact 400 infrared spectrometer using a DTGS detector. The Raman spectra in the liquid state were measured with a JASCO NR-1800 Raman spectrometer equipped with a

Princeton Instruments CCD detector. The 514.5 nm line of an NEC GLG 2162 argon ion laser was used for Raman excitation.

2.3 Calculations

Ab initio MO calculations of the energies and the optimized structural parameters were performed on all of the 14 possible conformers of MTE, shown in Figure 2.1, by the restricted Hartree–Fock (RHF) method using the 6-31G and 6-31G** basis sets and on the most stable four conformers by the second-order Møller–Plesset (MP2) perturbation theory using the 6-31G* basis set. The MO calculations were carried out by using the Gaussian 92 program[16] at the Computer Center of the Institute for Molecular Science, Okazaki, and the Gaussian 94 program[17] at the Information Processing Center of Hiroshima University.

Normal coordinate analysis was carried out with the NCTB program[18] at the Computer Center of the University of Tokyo on the 14 conformers of MTE on the basis of the ab initio MO calculations by the RHF method using the 6-31G basis set with the transferred scale factors[8] that conform to the Scaled Quantum Mechanical method.[19] The force constants in the Cartesian coordinate space obtained by the ab initio MO calculations were transformed into the group coordinate force constants.[20,21] The normal coordinate analysis based on the MP2 calculations with the 6-31G* basis set was also performed on the most stable four conformers of MTE by utilizing a uniform scale factor of 0.95.

2.4 Results and Discussion

2.4.1 Energies of Conformers

The relative energies of the conformers of MTE calculated at the RHF/6-31G, RHF/6-31G**, and MP2/6-31G* levels are given in Table 2.1, where the intramolecular interactions involved are indicated for the relevant conformers. The correlation diagram of the energies for the conformational states between

29
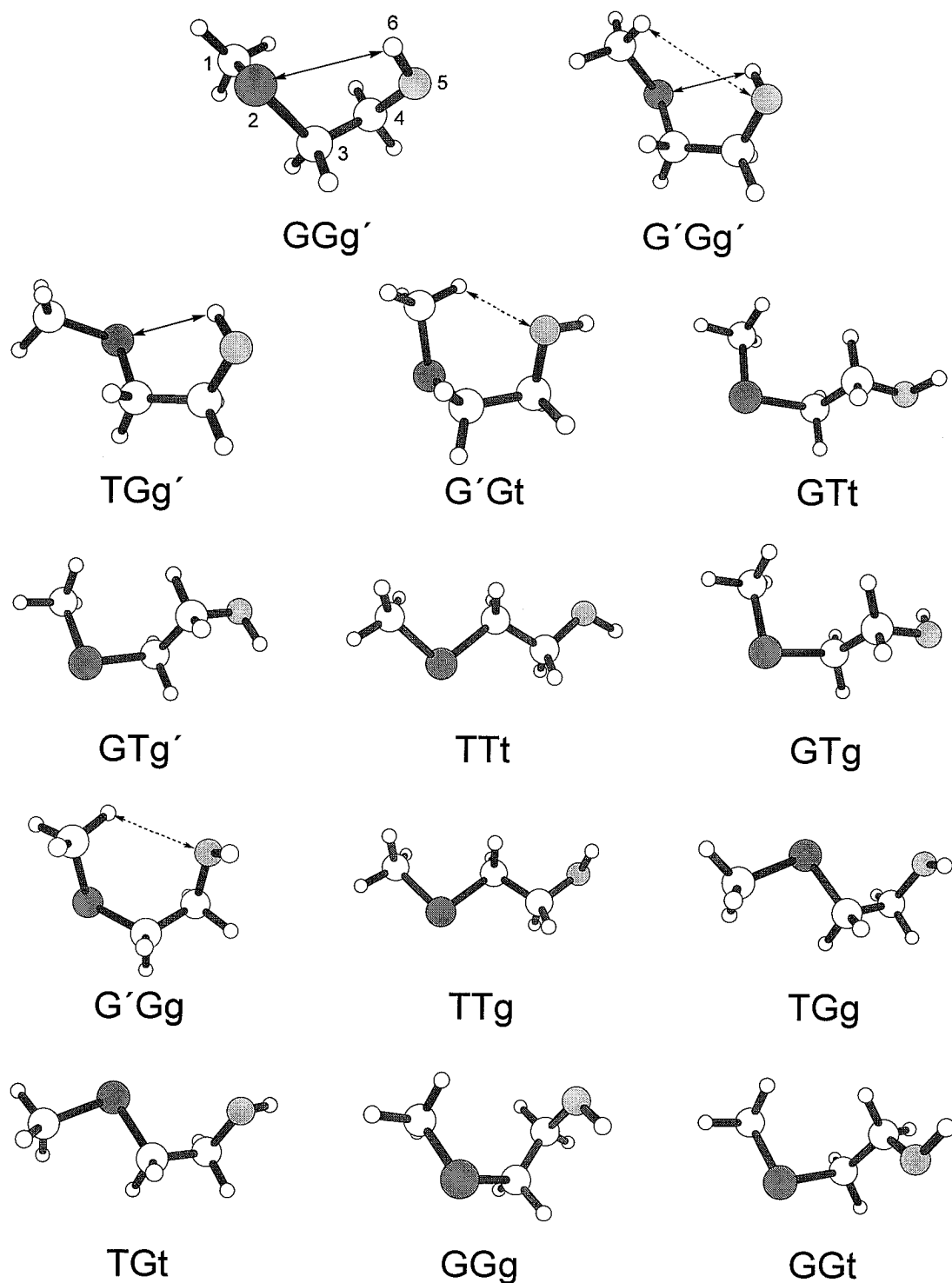
Figure 2.1 Optimized structures of 14 possible conformers of
2-(methylthio)ethanol. The solid arrows indicate intramolecular
OH···S hydrogen bonding and the dashed arrows indicate
intramolecular 1,5-CH···O interaction.

Table 2.1 Relative Energies of 14 Possible Conformers of 2-(Methylthio)ethanol Calculated by Various Methods

conformer	relative energy[a]/kJ mol^{-1}			interactions involved[b]
	RHF/6-31G	RHF/6-31G**	MP2/6-31G*	
GGg′	0.000	0.000	0.000	OH···S
G′Gg′	0.590	2.229	1.569	OH···S, CH···O
TGg′	1.775	2.873	4.377	OH···S
G′Gt	1.307	4.804	7.387	CH···O
GTt	4.268	5.641		
GTg′	5.641	5.825		
TTt	5.523	6.828		
GTg	7.443	7.013		
G′Gg	6.398	7.239		CH···O
TTg	7.863	7.542		
TGg	12.690	9.837		
TGt	11.783	10.726		
GGg	10.417	10.844		
GGt	12.529	12.146		

[a] Relative energy with respect to the energy for the GGg′ conformer. [b] OH···S, intramolecular OH···S hydrogen bonding; CH···O, intramolecular 1,5-CH···O interaction.

31
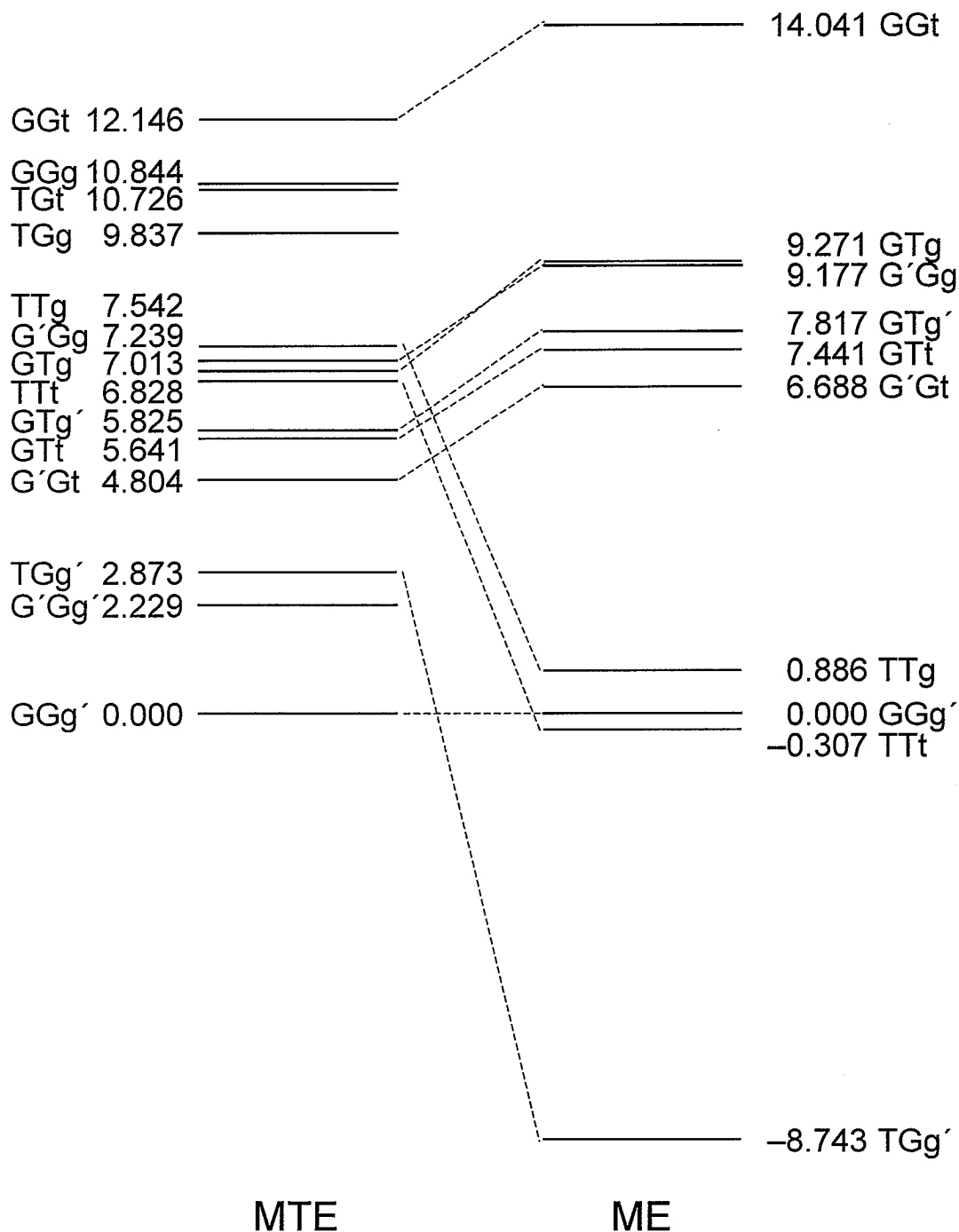
Figure 2.2 Correlation diagram of the energies for the conformational states between 2-(methylthio)ethanol (MTE) and 2-methoxyethanol (ME). The relative energies calculated at the RHF/6-31G** level are shown in units of kJ mol^{-1} with respect to the energy for the GGg′ conformer. The energies for 2-methoxyethanol are taken from ref 8; for the G′Gg′, TGg, TGt, and GGg conformers, minimum energy geometries were not attained.

MTE and ME is shown in Figure 2.2. The molecular conformation is designated by using the generic symbols[22] T or t for trans, G or g for gauche$^{\pm}$, and G' or g' for gauche$^{\mp}$; the lower-case symbols apply to the conformation around the CC–OH bond.

The most stable three conformers of MTE, namely GGg', G'Gg', and TGg', are obviously stabilized by intramolecular hydrogen bonding between the hydroxyl hydrogen atom and the sulfur atom, and the energy differences between these conformers are less than 3.0 kJ mol^{-1}. These results show that intramolecular OH···S hydrogen bonding is a dominant factor of the conformational stabilization of the MTE molecule.

The correlation diagram of the energies calculated at the RHF/6-31G** level indicates that the relative energies for the all conformers of MTE lie within 13 kJ mol^{-1}, but those for the conformers of ME range over more than 20 kJ mol^{-1}.[8] These calculated results show that this difference in the conformational stability between MTE and ME is associated primarily with the different intrinsic conformational preference of the CS–CC and CO–CC bonds; the gauche conformation is more stable than the trans conformation for the CS–CC bond by less than 2.0 kJ mol^{-1}, whereas the trans conformation is more stable than the gauche conformation for the CO–CC bond by more than 7.0 kJ mol^{-1}. The effect of intramolecular interactions involved in MTE on the molecular conformation will be discussed later in some detail.

2.4.2 Matrix-Isolation Infrared Spectra and Molecular Conformation

Figure 2.3 shows the infrared spectra of MTE in an argon matrix with Ar/MTE = 4000 at various temperatures during the heating process. The spectra were analyzed on the basis of normal coordinate analysis. For examining the molecular conformation of MTE, the C–S stretching vibrations are of great use, since their wavenumbers are sensitive to the conformation in the vicinity of the C–S bond.[23] In the 600–800 cm^{-1} region of the matrix-isolation spectra at 11 K, only one well-defined band is observed at 656 cm^{-1}. On the basis of the established correlation between the C–S stretching wavenumbers and the
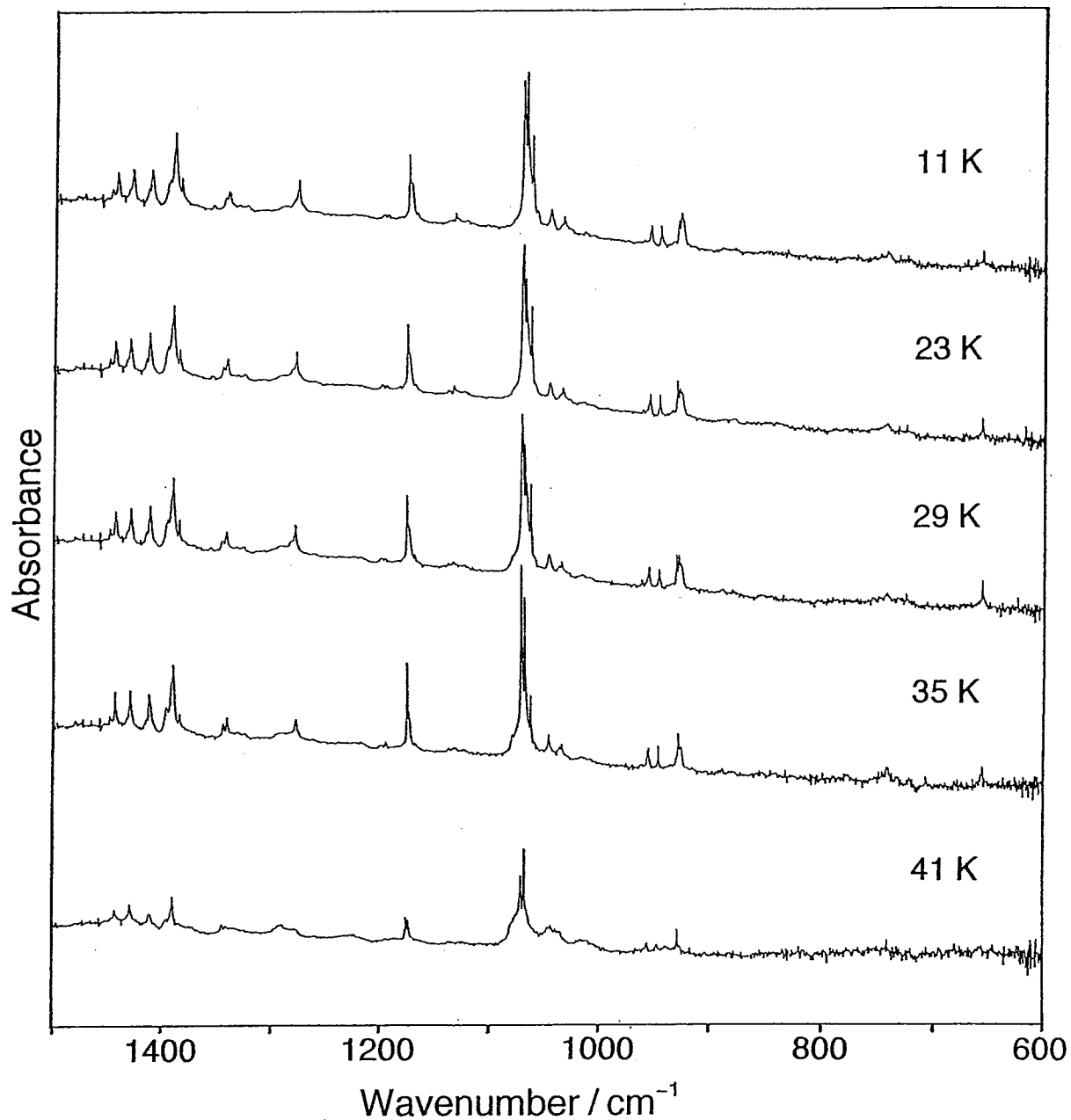
Figure 2.3 Infrared spectra of 2-(methylthio)ethanol in an argon matrix with Ar/MTE = 4000. The sample was deposited at 11 K and annealed at 23, 29, 35, and 41 K.

34

Table 2.2 Observed and Calculated Wavenumbers[a] and Vibrational Assignments for the GGg′ Conformer of 2-(Methylthio)ethanol

ν_{obs}[b]/cm^{-1}	ν_{calc}/cm^{-1} MP2/6-31G*[c]	ν_{calc}/cm^{-1} RHF/6-31G[d]	vibrational assignment[e]
3537 m	3537	3616	O–H stretch (100)
1482 vw	1496	1471	C_bH_2 scissor (100)
1443 m	1471	1441	CH_3 asym deform (91)
1430 m	1454	1435	CH_3 asym deform (89)
1412 m	1433	1417	C_aH_2 scissor (96)
1395 w, 1390 s	1387	1369	C_bH_2 wag (71), C–O–H bend (21)
1345 w, 1341 w	1369	1344	C–O–H bend (33), C_bH_2 wag (23)
1332 vw	1348	1326	CH_3 sym deform (100)
1278 m	1299	1279	C_aH_2 wag (71), C_bH_2 twist (16)
1195 vw	1201	1190	C_aH_2 twist (57), C–C stretch (10)
1177 s, 1174 m	1162	1151	C_bH_2 twist (54), C–O–H bend (18)
1072 s, 1069 s	1070	1081	C–O stretch (52), C–C stretch (36)
1047 w	1055	1062	CH_3 rock (25), C_aH_2 rock (20)
958 w, 957 w	979	986	CH_3 rock (89)
948 w	961	976	CH_3 rock (46), C_bH_2 rock (26)
929 m, 927 m	929	945	C–C stretch (26), C_bH_2 rock (21)
	820	837	C_aH_2 rock (53), C–O stretch (19)
	734	726	CH_3–S stretch (90), C–S stretch (14)
656 w	659	645	C–S stretch (80), CH_3–S stretch (18)
	469	472	C–C–O bend (62), C–C–S bend (21)
	420	338	C–O torsion (98)
	323	304	C–S–C bend (37), C–C–S bend (26)
	222	210	C–S–C bend (63), C–C–S bend (30)
	181	135	C–C torsion (56), CH_3–S torsion (27)
	141	111	CH_3–S torsion (68), C–C torsion (32)
	68	56	S–C torsion (110), C–O torsion (18)

[a] The CH_3 and CH_2 stretching vibrations are omitted from the table. [b] Observed wavenumbers for an argon matrix. Approximate relative intensities: s, strong; m, medium; w, weak; vw, very weak; sh, shoulder. [c] All wavenumbers have been scaled by a uniform factor of 0.95. [d] Wavenumbers have been scaled by the Scaled Quantum Mechanical method (see text). [e] Vibrational assignment for $CH_3SC_aH_2C_bH_2OH$ is given in terms of the group coordinates; sym, symmetric; asym, asymmetric. Potential energy distributions (%) evaluated from the RHF/6-31G calculations are shown in parentheses.

Table 2.3 Observed and Calculated Wavenumbers[a] and Vibrational Assignments for the G'Gg' Conformer of 2-(Methylthio)ethanol

v_{obs}[b]/cm^{-1}	v_{calc}/cm^{-1}		vibrational assignment[e]
	MP2/6-31G*[c]	RHF/6-31G[d]	
3549 w	3552	3628	O–H stretch (100)
	1486	1465	C_bH_2 scissor (100)
1448 w	1482	1448	CH_3 asym deform (95)
1433 sh	1455	1434	CH_3 asym deform (95)
1415 w	1438	1421	C_aH_2 scissor (95)
1386 w	1381	1364	C_bH_2 wag (96)
1355 vw	1363	1355	C–O–H bend (52), C_bH_2 twist (23)
1324 vw	1358	1325	CH_3 sym deform (100)
1282 sh	1299	1280	C_aH_2 wag (65), C_bH_2 twist (17)
1200 vw	1208	1201	C_aH_2 twist (41), C_aH_2 wag (19)
1170 vw	1160	1146	C_bH_2 twist (40), C_aH_2 twist (27)
1064 s	1063	1073	C–O stretch (55), C–C stretch (34)
1035 w	1041	1052	CH_3 rock (32), C_aH_2 rock (18)
963 vw	986	994	CH_3 rock (91)
	970	979	CH_3 rock (46), C_bH_2 rock (26)
932 m	927	945	C–O stretch (24), C–C stretch (24)
	812	834	C_aH_2 rock (53), C–O stretch (17)
	729	720	CH_3–S stretch (91), C–S stretch (14)
656 w	674	660	C–S stretch (75), CH_3–S stretch (17)
	463	470	C–C–O bend (62), C_aH_2 rock (21)
	438	319	C–O torsion (107)
	292	271	C–S–C bend (42), C–C–S bend (33)
	243	239	C–S–C bend (52), C–C–S bend (35)
	174	130	CH_3–S torsion (98)
	139	110	C–C torsion (95), C–O torsion (10)
	104	66	S–C torsion (175), C–O torsion (26)

[a–e] See footnotes a–e, respectively, of Table 2.2.
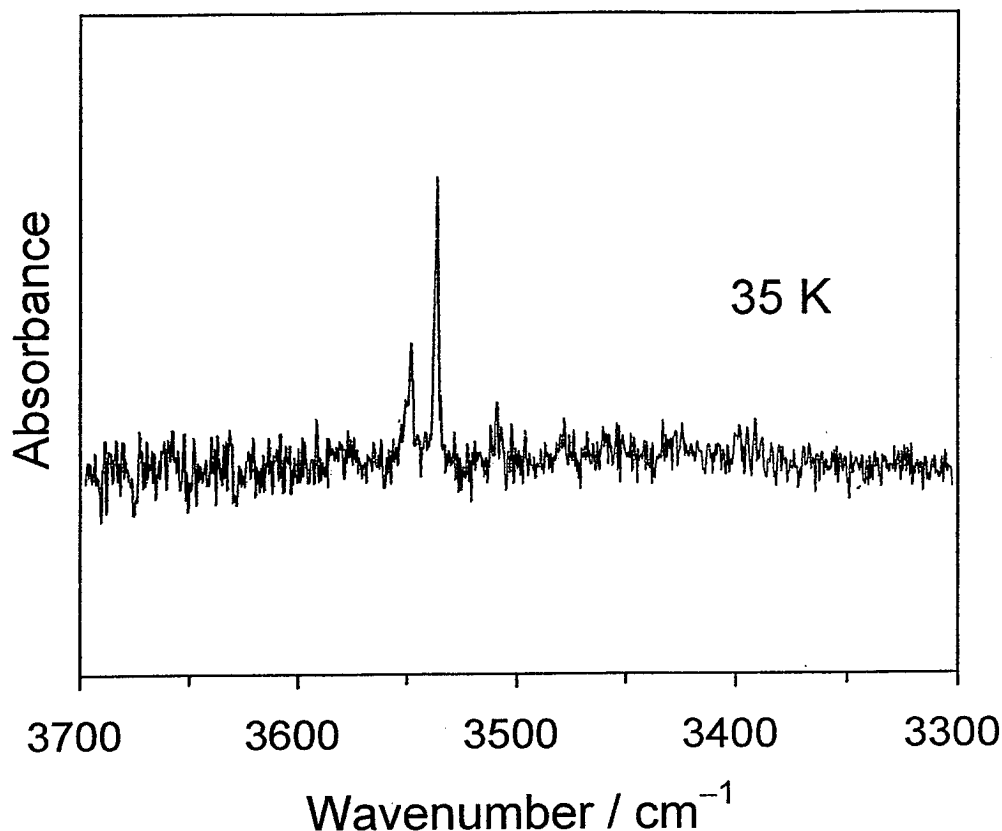
Figure 2.4 Infrared spectrum of 2-(methylthio)ethanol in an argon matrix with Ar/MTE = 4000 at 35 K in the region of O–H stretching vibrations.

conformation,[23] this band is assigned to the S–C(H_2) stretching vibration of the gauche$^{\pm}$–gauche$^{\pm}$ and gauche$^{\mp}$–gauche$^{\pm}$ conformations around CS–C–CO bonds. This matrix-isolation band corresponds to the Raman band at 655 cm^{-1} observed for liquid MTE, which is assigned decisively to the above conformations as will be described later. This observation of the matrix-isolation spectra implies that the conformers existing in the matrix are GGx and/or G′Gx, where x denotes either of t, g, and g′.

In the spectral region of the O–H stretching vibrations, two bands are observed at 3537 and 3549 cm^{-1} in the argon matrix (Figure 2.4). These bands are associated with intramolecularly hydrogen-bonded O–H stretching vibrations, and their wavenumbers are in excellent agreement with the calculated

wavenumbers by the MP2 method, 3537 cm^{-1} for the GGg′ conformer and 3552 cm^{-1} for the G′Gg′ conformer, respectively. The matrix-isolation spectra exhibit, however, no bands that are assignable to free O–H stretching vibrations.

The results of normal coordinate analysis further show that all of the bands observed in an argon matrix at 11 K are assigned consistently to the two conformers, GGg′ and G′Gg′, but not assigned to any others. The calculated wavenumbers and vibrational assignments for these conformers, together with the observed wavenumbers, are given in Tables 2.2 and 2.3. The discriminated assignments of the observed bands to the GGg′ and G′Gg′ conformers are consistent with the observed intensity behavior with increasing temperature. It may be remarked that most of the matrix-isolation bands associated with the GGg′ conformer are observed in doublet, while those associated with the G′Gg′ conformer are observed in singlet. The origin of the doublet for the GGg′ conformer is not clear from the present analysis. The spectral evidence for the predominant existence of the GGg′ and G′Gg′ conformers in the matrix-isolated state agrees with the theoretical prediction from the calculated energies (Table 2.1).

On heating the matrix sample up to 29 K, the bands due to the G′Gg′ conformer, such as a prominent band at 1064 cm^{-1}, decrease in intensity, while the bands due to the GGg′ conformer persist in the matrix (Figure 2.3). This spectral observation indicates that the GGg′ conformer is the most stable in an argon matrix, since the annealing process induces a transformation of less stable conformers trapped in the matrix at lower temperatures into the most stable conformer. These experimental results are again in agreement with the calculated energies.

In a previous microwave spectroscopic study of MTE,[11] only the GGg′ conformer was identified in the gas phase.[24] This study has confirmed the existence of the second most stable conformer of G′Gg′ in an argon matrix. Both of the GGg′ and G′Gg′ conformers are stabilized by intramolecular OH⋯S hydrogen bonding, and the latter conformer is additionally stabilized by 1,5-CH⋯O interaction although this form assumes a sterically unfavorable G′G conformation in the $CH_3S-CH_2-CH_2O$ group. The implications of the

intramolecular interactions in the conformational stabilization will be discussed later.

At temperatures higher than about 40 K, all of the persisting bands become significantly weaker, and broad features grow instead in the spectra, which are ascribed to the aggregates of the molecules produced by the loosening of the matrix lattice in a heating process. Since some of the broad bands are not assignable to either of the GGg′ and G′Gg′ conformers, it is obvious that the molecular aggregation accompanies conformational changes. The previous study on ME[8] has shown that the conformation around the CO–C–COH bonds being trans–gauche is maintained on molecular aggregation. For MTE, on the other hand, the molecules can adopt various possible conformations around the CS–C–COH bonds on aggregation, since the energies of most of the conformers lie within 8 kJ mol^{-1} (Table 2.1 and Figure 2.2).

2.4.3 Infrared and Raman Spectra in the Condensed Phases

The infrared spectra of MTE in the liquid and glassy states are shown in Figure 2.5, where the matrix-isolation infrared spectrum at 41 K is also shown for comparison. The spectra of the liquid and glassy states are significantly different from the spectra of the isolated and aggregated states in an argon matrix. In the liquid state, additional bands, not observed in an argon matrix at low temperatures, are noted at 1045, 1011, 786, 766, and 700 cm^{-1}. The appearance of these bands suggests the coexistence of various conformers in these condensed phases.

The Raman spectrum in the 600–800 cm^{-1} region of MTE in the liquid state is shown in Figure 2.6, where the C–S stretching bands are observed. Since the C–S stretching wavenumbers are sensitive to the conformation,[23] these bands provide important information about the skeletal conformation of the MTE molecule. The wavenumbers and conformational assignments of the C–S stretching bands for liquid MTE are given in Table 2.4. The strong band at 701 cm^{-1} is assigned to the gauche–trans conformation around the CS–C–COH bonds and the weaker bands at 676 and 771 cm^{-1} are assigned to the trans–gauche and
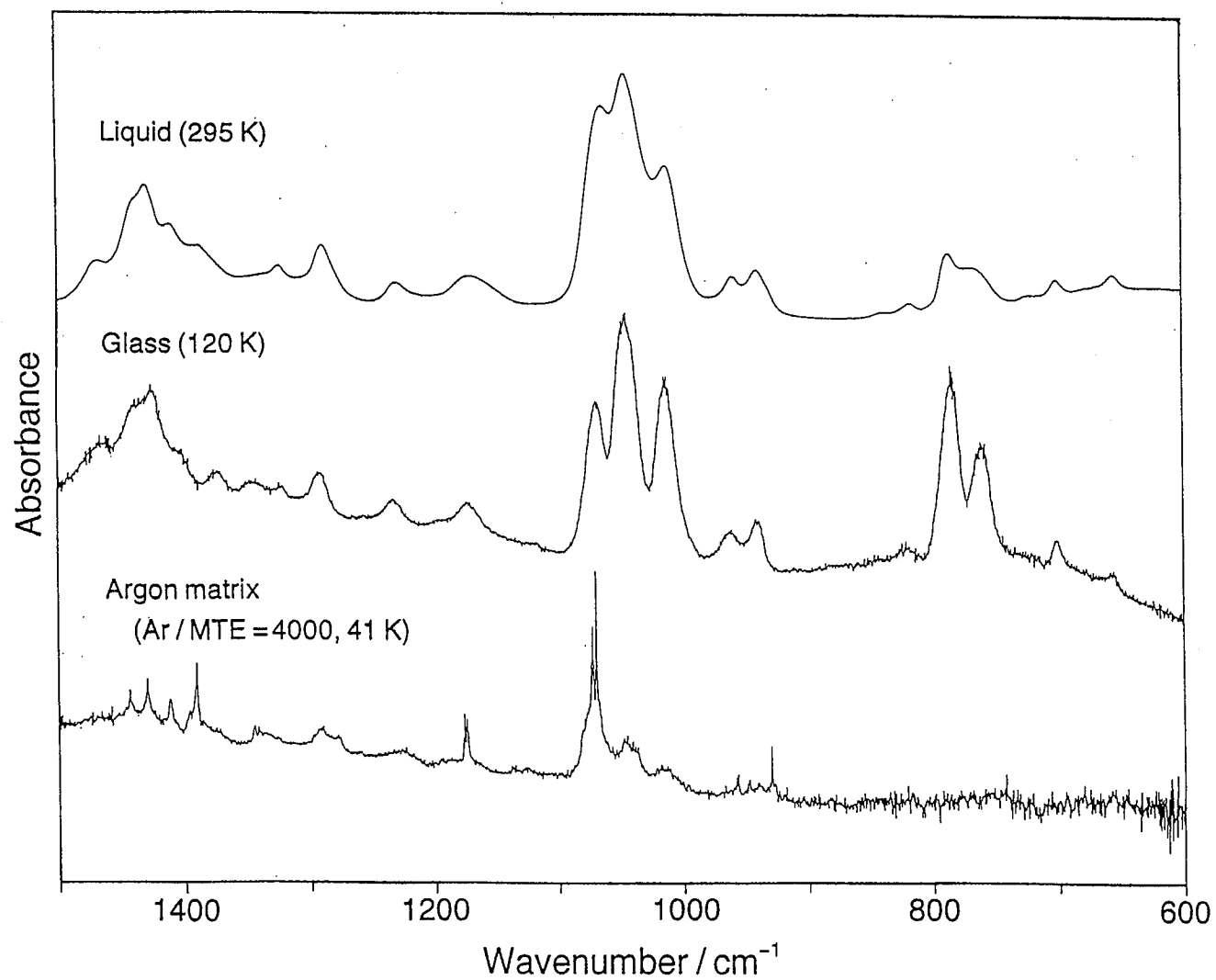
Figure 2.5 Infrared spectra of 2-(methylthio)ethanol in the liquid state at 295 K, the glassy state at 120 K, and the aggregated state in an argon matrix with Ar/MTE = 4000 at 41 K.

Table 2.4 Observed and Calculated Wavenumbers of the C–S Stretching Vibrations for 2-(Methylthio)ethanol

$\nu_{obs}{}^{b}$/cm^{-1}	$\nu_{calc}{}^{a}$/cm^{-1}									
	GGg′	G′Gg′	TGg′	G′Gt	GTt	GTg′	TTt	GTg	G′Gg	TTg
771 w							776			780
752 vw					771	778		778		
724 m	726	720	730	725					725	
715 sh							719			719
701 s					700	699		700		
676 w			662							
655 s	645	660		658					650	

^{a} Calculated by the RHF/6-31G method. ^{b} Observed wavenumbers in the Raman spectrum in the liquid state. For approximate relative intensities, see footnote b of Table 2.2.
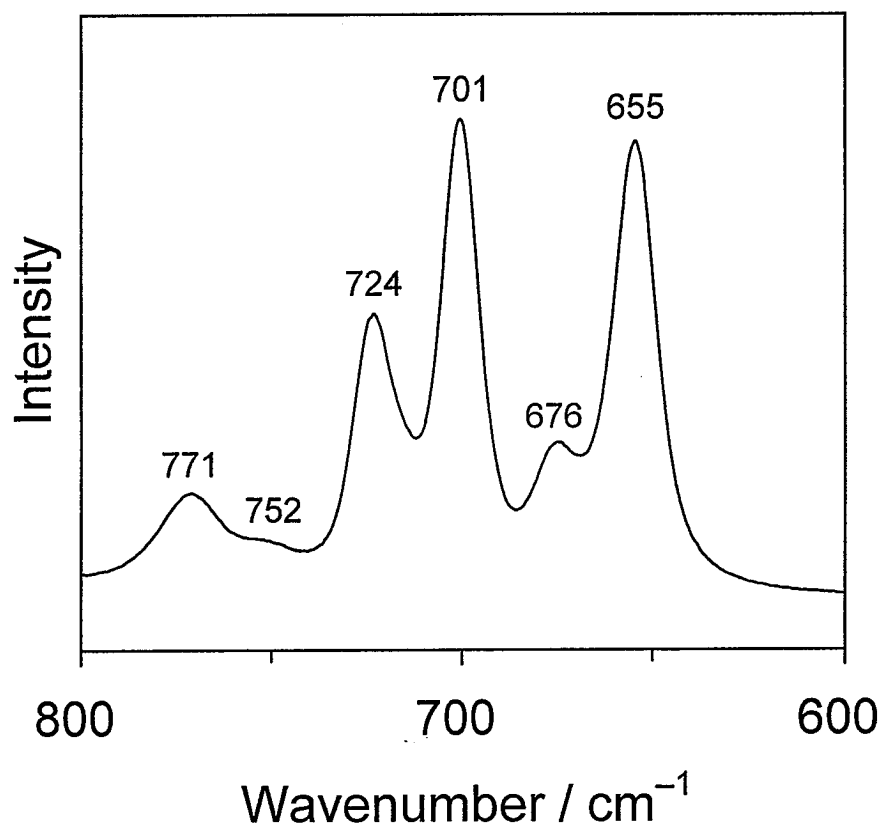
Figure 2.6 Raman spectrum of 2-(methylthio)ethanol in the liquid state at 295 K.

trans–trans conformations, respectively. These Raman spectral observations indicate that there exist a number of conformers, GGx, G′Gx, TGx, GTx, and TTx, in the liquid state. The orientation of the hydroxyl group is not clear in the condensed phases because of complicated intermolecular hydrogen bonding in these phases.

2.4.4 Intramolecular OH···S and CH···O Interactions and Structural Parameters

In the conformational stabilization of the MTE molecule, two types of intramolecular interactions are involved; one is OH···S hydrogen bonding and the other is 1,5-CH···O interaction. These interactions are discussed below in relation to the energies and the structural parameters for the relevant conformers.

The optimized structural parameters for 14 conformers of MTE calculated at the RHF/6-31G** level are given in Table 2.5. Numbering of atoms for the MTE molecule is shown in Figure 2.1, where the intramolecular interactions in question are indicated by arrows.

The ab initio MO calculations of the energies show that OH···S hydrogen bonding stabilizes to a great extent the XGg' conformers, where X is either of T, G, and G'. The matrix-isolation infrared spectra of MTE have in fact evidenced the theoretical prediction that the GGg' conformer is the most stable and the G'Gg' conformer is the second most stable. The relative strength of intramolecular OH···S hydrogen bonding can be estimated from the nonbonded OH···S distance. Of the three relevant conformers GGg', G'Gg', and TGg', the first conformer has the shortest OH···S distance and the second conformer has the longest distance. These OH···S distances imply that the strength of intramolecular hydrogen bonding in these conformers is in order of GGg' > TGg' > G'Gg'. In accordance with this decreasing trend of the strength of the hydrogen bonding, the O–H bond length in these conformers decreases in the same order. The results in Table 2.5 indicate that the length of the O–H bond increases on the formation of intramolecular hydrogen bonding by roughly 0.002 Å.

It appeared difficult at first to understand the high stability of the G'Gg' conformer, for which the methyl group and the hydroxyl group come close to each other. This peculiar conformational property is explained by significant 1,5-CH···O interaction, which has been well-established to be an important factor to stabilize the gauche$^{\mp}$–gauche$^{\pm}$ conformation of the $CH_3O–CH_2–CH_2OCH_3$ structure of 1,2-dimethoxyethane.[13,14] It is remarked that the optimized geometry of the G'Gg' conformer of MTE is considerably distorted so that the C–S–C–C torsion angle, $\mp96.6°$, is deviated greatly from the normal gauche$^{\mp}$ angle of $\mp60°$. This geometry is elucidated as a consequence of being a compromise configuration which is simultaneously accessible to both of OH···S hydrogen bonding and 1,5-CH···O interaction. Without being distorted, the methyl hydrogen atom and the hydroxyl hydrogen atom would be heavily hindered by each other. It is clear that this distorted geometry is not best suited for the

Table 2.5 Optimized Structural Parameters for 14 Conformers of 2-(Methylthio)ethanol Calculated by the RHF/6-31G** Method

structural parameters[a]	GGg'[b]	G'Gg'[b,c]	TGg'[b]	G'Gt[c]	GTt	GTg'	TTt
			Bond Lengths/Å				
C_1–H	1.0820	1.0808[d]	1.0821	1.0785[d]	1.0820	1.0818	1.0821
	1.0822	1.0824	1.0825	1.0827	1.0823	1.0823	1.0828
	1.0829	1.0825	1.0825	1.0830	1.0829	1.0828	1.0828
C_1–S_2	1.8109	1.8134	1.8084	1.8115	1.8109	1.8110	1.8081
S_2–C_3	1.8195	1.8227	1.8215	1.8159	1.8138	1.8145	1.8162
C_3–C_4	1.5247	1.5246	1.5252	1.5176	1.5192	1.5250	1.5189
C_4–O_5	1.3942	1.3978	1.3957	1.4020	1.4025	1.4012	1.4019
O_5–H_6	0.9447	0.9438	0.9442	0.9424	0.9427	0.9430	0.9427
			Bond Angles/deg				
C_1–S_2–C_3	101.56	101.27	100.93	102.52	101.65	101.60	99.90
S_2–C_3–C_4	114.25	113.61	110.49	115.68	114.03	114.21	110.43
C_3–C_4–O_5	112.57	113.02	112.73	109.17	107.08	111.41	106.99
C_4–O_5–H_6	109.17	108.77	109.59	109.93	109.98	109.90	109.82
			Torsion Angles/deg				
C_1–S_2–C_3–C_4	76.96	−96.58	−159.57	−81.18	79.03	76.94	180.00
S_2–C_3–C_4–O_5	62.31	58.09	69.59	69.31	−179.72	−178.16	180.00
C_3–C_4–O_5–H_6	−58.96	−74.51	−60.70	−174.14	−177.80	−70.97	180.00
			Nonbonded Interatomic Distances/Å				
C_1H⋯O_5		2.7899		2.5507			
$O_5$$H_6$⋯$S_2$	2.7770	2.8642	2.8066				

(Continued)

44

structural parameters[a]	GTg	G'Gg[c]	TTg	TGg	TGt	GGg	GGt
			Bond Lengths/Å				
C_1–H	1.0819	1.0787[d]	1.0821	1.0823	1.0824	1.0814	1.0825
	1.0823	1.0826	1.0827	1.0833	1.0832	1.0823	1.0828
	1.0832	1.0837	1.0829	1.0833	1.0834	1.0833	1.0834
C_1–S_2	1.8109	1.8113	1.8083	1.8085	1.8084	1.8083	1.8096
S_2–C_3	1.8144	1.8151	1.8161	1.8170	1.8183	1.8152	1.8158
C_3–C_4	1.5249	1.5240	1.5253	1.5241	1.5173	1.5283	1.5192
C_4–O_5	1.4012	1.4012	1.4002	1.3966	1.3989	1.3943	1.3976
O_5–H_6	0.9429	0.9431	0.9429	0.9433	0.9423	0.9432	0.9421
			Bond Angles/deg				
C_1–S_2–C_3	101.74	102.78	100.07	99.58	99.60	102.03	101.00
S_2–C_3–C_4	114.28	116.05	110.49	111.58	111.62	116.49	115.54
C_3–C_4–O_5	111.38	113.55	111.29	113.62	108.85	114.76	108.54
C_4–O_5–H_6	110.03	109.79	109.88	110.21	110.09	110.48	110.22
			Torsion Angles/deg				
C_1–S_2–C_3–C_4	77.79	–75.43	–178.40	169.80	167.36	52.61	80.18
S_2–C_3–C_4–O_5	176.69	68.44	–181.42	56.72	64.92	46.98	69.62
C_3–C_4–O_5–H_6	70.78	70.56	72.10	57.36	189.19	44.56	–169.53
			Nonbonded Interatomic Distances/Å				
$C_1H\cdots O_5$		2.5740					
$O_5H_6\cdots S_2$							

[a] For numbering of atoms, see Figure 2.1. [b] Conformer in which the intramolecular OH···S hydrogen bonding is involved. [c] Conformer in which the intramolecular 1,5-CH···O interaction is involved. [d] C–H bond associated with the intramolecular 1,5-CH···O interaction.

45

respective interactions to be the most effective. This is the reason why the hydrogen bonding in the G′Gg′ conformer is not so strong as in GGg′ or TGg′ for which no such complication is involved.

For ME, intramolecular OH···O hydrogen bonding, which is analogous to OH···S hydrogen bonding in MTE, stabilizes the TGg′ and GGg′ conformers, but the G′Gg′ conformer failed to be appropriately optimized in the ab initio MO calculation.[8,25] The optimization of the G′Gg′ conformation actually resulted in the conversion into the TGg′ conformation with an increased C–O–C–C torsion angle, being consistent with the result that the trans conformation around the CO–CC bond is significantly more stable than the gauche conformation.

The intramolecular 1,5-CH···O interaction is important for the stabilization of the G′Gg′ conformer of MTE, as described above, and other conformers in which the gauche$^{\mp}$–gauche$^{\pm}$ conformation of the CH_3S–CH_2–CH_2OH structure is involved, namely the G′Gt and G′Gg conformers. The relative strength of this interaction can be estimated from the relevant nonbonded CH···O distance. According to the results in Table 2.5, this distance is the shortest for G′Gt and is the longest for G′Gg′ among the three conformers. This implies that the strength of the 1,5-CH···O interaction is in order of G′Gt > G′Gg > G′Gg′. In conformity with this decreasing trend, the length of the methyl C–H bond associated with this interaction increases in the same order. It is remarked that the length of the C–H bond decreases when it is involved in the CH···O interaction, while the length of the O–H bond increases when it is involved in hydrogen bonding. The present finding that the relative strength of 1,5-CH···O interaction is the least for G′Gg′ among the three G′Gx conformers is again consistent with the distorted geometry of this conformation, which is not best suited for this interaction to be the most effective. In the G′Gg′ conformer, the two intramolecular interactions involved, namely OH···S hydrogen bonding and 1,5-CH···O interaction, are competing in the conformational stabilization of this form, leading to the heavy geometrical constraint and accordingly to the diminished effect of the respective interactions.

In a previous study,[12] Gil et al. have discussed on the basis of ab initio MO calculations the conformational stability of the $CH_3XCH_2CH_2YH$ molecules,

where X and Y are O or S. They focused on the effect of intramolecular YH⋯X hydrogen bonding on the conformation in a series of the analogous compounds. This study has clarified the importance of intramolecular 1,5-CH⋯O interaction as well in the conformational stabilization of the MTE molecule. This interaction should also be important for other $CH_3XCH_2CH_2YH$ compounds, but the previous authors did not consider in their calculations the conformational forms in which this interaction is involved.[12,26] In another work,[27] the authors have discussed a different type of intramolecular CH⋯O interaction relevant to the alkoxyl part of the $CH_3(CH_2)_{n-1}OCH_2CH_2OH$ molecules, where $n \geq 3$. This interaction has been found to be important for the stabilization of the gauche conformation around the CC–CO bond.[27]

The conformation of particular part of the MTE molecule is correlated with the structural parameters shown in Table 2.5. The XGg′ conformers, which are capable of forming intramolecular OH⋯S hydrogen bonding, have a longer O–H bond than the normal O–H bond as described before. In accordance with the increased O–H bond length in these conformers, the S–C(H₂) bond length is increased and the C–O–H angle is decreased as compared with those for other conformers. The methyl C–H bond in the G′Gx conformers, which is associated with 1,5-CH⋯O interaction, is shorter than other C–H bonds in the methyl group as mentioned above. It is noted that the C–C bond is longer for the conformers with the gauche CC–OH bond, but it is shorter for those with the trans bond. For the conformers with the trans CS–CC bond, the C–S–C and S–C–C angles are smaller than those with the gauche bond.

2.5 Conclusions

Matrix-isolation infrared spectroscopy has clarified that the most stable conformer of MTE is GGg′ and the second most stable conformer is G′Gg′, in agreement with the energies calculated by the ab initio MO method. These conformers and the TGg′ conformer, which is the third most stable according to the calculation, are stabilized by intramolecular hydrogen bonding between the hydroxyl hydrogen atom and the sulfur atom. For the G′Gg′ conformer, in

which an additional intramolecular interaction between the methyl hydrogen atom and the hydroxyl oxygen atom is involved, the two interactions are competing in the conformational stabilization of this form, leading to the heavy geometrical constraint and accordingly to the diminished effect of the respective interactions. For ME, on the other hand, the G'Gg' conformation is unstable owing to strong preference of the trans conformation around the CO–CC bond. The present study emphasizes the importance of intramolecular interactions in the conformational stabilization of MTE and other relevant compounds.

References and Notes

(1) Frei, H.; Ha, T.-K.; Meyer, R.; Günthard, Hs. H. *Chem. Phys.* **1977**, *25*, 271–298.

(2) Takeuchi, H.; Tasumi, M. *Chem. Phys.* **1983**, *77*, 21–34.

(3) Park, G. G.; Tasumi, M. *J. Phys. Chem.* **1991**, *95*, 2757–2762.

(4) Iwamoto, R. *Spectrochim. Acta, Part A* **1971**, *27*, 2385–2399.

(5) Singelenberg, F. A. J.; van der Maas, J. H. *J. Mol. Struct.* **1991**, *243*, 111–122.

(6) Singelenberg, F. A. J.; Lutz, E. T. G.; van der Maas, J. H.; Jalsovszky, G. *J. Mol. Struct.* **1991**, *245*, 173–182.

(7) Singelenberg, F. A. J; van der Maas, J. H.; Kroon-Batenburg, L. M. J. *J. Mol. Struct.* **1991**, *245*, 183–194.

(8) Yoshida, H.; Takikawa, K.; Ohno, K.; Matsuura, H. *J. Mol. Struct.* **1993**, *299*, 141–147.

(9) Yoshida, H.; Takikawa, K.; Kaneko, I.; Matsuura, H. *J. Mol. Struct. (THEOCHEM)* **1994**, *311*, 205–210.

(10) Sung, E.-M.; Harmony, M. D. *J. Am. Chem. Soc.* **1977**, *99*, 5603–5608.

(11) Marstockk, K.-M.; Møllendal, H.; Uggerud, E. *Acta Chem. Scand.* **1989**, *43*, 26–31.

(12) Gil, F. P. S. C.; Amorim da Costa, A. M.; Teixeira-Dias, J. J. C. *J. Phys. Chem.* **1995**, *99*, 16586–16589.

(13) Yoshida, H.; Kaneko, I.; Matsuura, H.; Ogawa, Y.; Tasumi, M. *Chem. Phys. Lett.* **1992**, *196*, 601–606.

(14) Yoshida, H.; Tanaka, T.; Matsuura, H. *Chem. Lett.* **1996**, 637–638.

(15) Tsuzuki, S.; Uchimaru, T.; Tanabe, K.; Hirano, T. *J. Phys. Chem.* **1993**, *97*, 1346–1350.

(16) Frisch, M. J.; Trucks, G. W.; Head-Gordon, M.; Gill, P. M. W.; Wong, M. W.; Foresman, J. B.; Johnson, B. G.; Schlegel, H. B.; Robb, M. A.; Replogle, E. S.; Gomperts, R.; Andres, J. L.; Raghavachari, K.; Binkley, J. S.; Gonzalez, C.; Marin, R. L.; Fox, D. J.; Defrees, D. J.; Baker, J.; Stewart, J. J. P.; Pople, J. A. *Gaussian 92*, Revision F.3; Gaussian Inc., Pittsburgh, PA, 1992.

(17) Frisch, M. J.; Trucks, G. W.; Schlegel, H. B.; Gill, P. M. W.; Johnson, B. G.; Robb, M. A.; Cheeseman, J. R.; Keith, T.; Petersson, G. A.; Montgomery, J. A.; Raghavachari, K.; Al-Laham, M. A.; Zakrzewski, V. G.; Ortiz, J. V.; Foresman, J. B.; Cioslowski, J.; Stefanov, B. B.; Nanayakkara, A.; Challacombe, M.; Peng, C. Y.; Ayala, P. Y.; Chen, W.; Wong, M. W.; Andres, J. L.; Replogle, E. S.; Gomperts, R.; Martin, R. L.; Fox, D. J.; Binkley, J. S.; Defrees, D. J.; Baker, J.; Stewart, J. P.; Head-Gordon, M.; Gonzalez, C.; Pople, J. A. *Gaussian 94*, Revision D.3; Gaussian Inc., Pittsburgh, PA, 1995.

(18) Shimanouchi, T. *Computer Programs for Normal Coordinate Treatment of Polyatomic Molecules*; The University of Tokyo, 1968.

(19) Pulay, P.; Fogarasi, G.; Pongor, G.; Boggs, J. E.; Vargha, A. *J. Am. Chem. Soc.* **1983**, *105*, 7037–7047.

(20) Matsuura, H.; Tasumi, M. In *Vibrational Spectra and Structure*; Durig, J. R., Ed.; Elsevier: Amsterdam, 1983; pp 69–143.

(21) Yoshida, H.; Tasumi, M. *J. Chem. Phys.* **1988**, *89*, 2803–2809.

(22) Shimanouchi, T.; Ogawa, Y.; Ohta, M.; Matsuura, H.; Harada, I. *Bull. Chem. Soc. Jpn.* **1976**, *49*, 2999–3008.

(23) Nogami, N.; Sugeta, H.; Miyazawa, T. *Bull. Chem. Soc. Jpn.* **1975**, *48*, 2417–2420.

(24) This conformation was denoted as GGg in the original paper,[11] but it should be designated properly as GGg′ in accord with the geometrical structure actually determined.

(25) The RHF/6-31G** calculations on the G′Gg′ and GGg conformers of ME, which had not been treated in the previous study,[8] were performed in this work for comparison with the results for the corresponding conformers of MTE.

(26) Gil, F. P. S. C.; Fausto, R.; Amorim da Costa, A. M.; Teixeira-Dias, J. J. C. *J. Chem. Soc., Faraday Trans.* **1994**, *90*, 689–695.

(27) Gil, F. P. S. C.; Amorim da Costa, A. M.; Teixeira-Dias, J. J. C. *J. Phys. Chem.* **1995**, *99*, 8066–8070.

Chapter 3

Density Functional Studies on Conformational and Vibrational Analyses of 2-(Methylthio)ethanol

Abstract

Conformational and vibrational analyses were performed on 2-methoxyethanol (ME) and 2-(methylthio)ethanol (MTE) by density functional theory (DFT). The energies, molecular geometries and vibrational wavenumbers were calculated for the TGg′, GGg′, TTt, and TGt conformers of ME and the GGg′, G′Gg′, TGg′, and GGt conformers of MTE by the BLYP, B3LYP, and B3PW91 methods using the 6-31G* basis set. The calculations by the HF and MP2 methods were also carried out on the same conformers. The calculated energies are consistent with the experimental findings that the TGg′ conformer of ME and the GGg′ and G′Gg′ conformers of MTE are present in a low-temperature matrix. The DFT calculations give the stabilization energy by OH⋯S hydrogen bonding substantially the same as the stabilization energy by OH⋯O hydrogen bonding. The vibrational wavenumbers for the TGg′ conformer of ME and the GGg′ conformer of MTE are successfully predicted by the MP2, B3LYP, and B3PW91 methods using uniform scale factors for the respective methods. The experimental large wavenumber difference between ME and MTE of the intramolecular hydrogen bonded O–H stretching vibrations is reproduced much better with the DFT calculations than with the ab initio molecular orbital calculations. This study has shown that Becke's three-parameter hybrid functional methods overall give the most accurate results.

3.1 Introduction

The structure of isolated molecules is determined by a number of factors that include various intramolecular interactions.[1] The most important intramolecular interaction is intramolecular hydrogen bonding,[2,3] which is well known to stabilize particular conformations of many organic and biologically important molecules. One of the other important interactions is an intramolecular 1,5-CH$\cdots$O interaction, which has been found to be remarkable in the conformational stabilization of 1,2-dimethoxyethane, $CH_3OCH_2CH_2OCH_3$, as revealed by experimental[4–6] and theoretical[7–13] studies. The results of these studies have indicated that, although this interaction is generally weaker than hydrogen bonding, its effect may be dominant in cases where hydrogen bonding is not important. This attractive interaction may be called CH$\cdots$O hydrogen bonding, being similar to what have been found in organic crystals.[14]

In the previous studies,[15,16] the conformational stabilities of 2-(methylthio)ethanol (MTE), $CH_3SCH_2CH_2OH$, and 2-methoxyethanol (ME), $CH_3OCH_2CH_2OH$, have been investigated by matrix-isolation infrared spectroscopy and ab initio molecular orbital (MO) calculations. These studies have shown that intramolecular OH$\cdots$S or OH$\cdots$O hydrogen bonding plays an important role in the conformational stabilization and that the O–H stretching wavenumber for MTE associated with OH$\cdots$S hydrogen bonding is significantly lower than the wavenumber for ME associated with OH$\cdots$O hydrogen bonding.

In this work, conformational and vibrational analyses of ME and MTE have been performed by using density functional theory (DFT),[17] which has been shown to reproduce with high accuracy the experimental molecular geometries and vibrational wavenumbers for many organic compounds.[18–20] On the basis of the results of DFT calculations, the conformational stabilization by intramolecular hydrogen bonding and the wavenumbers of the O–H stretching vibrations are discussed.

3.2 Calculations

The DFT calculations were performed on three conformers of ME, namely trans–gauche$^\pm$–gauche$^\mp$ (TGg'), gauche$^\pm$–gauche$^\pm$–gauche$^\mp$ (GGg') and trans–trans–trans (TTt) around the $CH_3O–CH_2–CH_2–OH$ bonds, and three conformers of MTE, gauche$^\pm$–gauche$^\pm$–gauche$^\mp$ (GGg'), gauche$^\mp$–gauche$^\pm$–gauche$^\mp$ (G'Gg') and trans–gauche$^\pm$–gauche$^\mp$ (TGg') around the $CH_3S–CH_2–CH_2–OH$ bonds. These conformers, shown in Figures 3.1 and 3.2, were selected for the present calculations, because the previous Hartree–Fock (HF) calculations using the 6-31G** basis set revealed that they are the lowest-energy three conformers of ME and MTE.[15,16] The DFT calculations were also performed on the trans–gauche$^\pm$–trans (TGt) conformer of ME and the gauche$^\pm$–gauche$^\pm$–trans (GGt) conformer of MTE in order to estimate the stabilization energy by intramolecular hydrogen bonding.

In the present DFT calculations, the 6-31G* basis set and the following functionals are used: the Becke hybrid functional[21] coupled with the correlation functional of Lee, Yang and Parr[22] (BLYP), Becke's three-parameter hybrid functional[23] in combination with the LYP correlation functional (B3LYP) and Becke's three-parameter hybrid functional in combination with the correlation functional of Perdew and Wang[24-26] (B3PW91). The HF calculations using the same basis set were also performed on the relevant conformers in order to compare the results with those from the DFT calculations. In addition, the Møller–Plesset (MP2) calculations were carried out on ME by using the 6-31G* basis set; the same calculations on MTE were described in Chapter 2.[15]

The computation was carried out with the Gaussian 94 program[27] at the Information Processing Center of Hiroshima University. For the calculations with this program, the default parameters were used. Normal coordinate calculations were performed by using uniform wavenumber scale factors for the respective force fields; namely 1.00 for BLYP, 0.97 for B3LYP, 0.97 for B3PW91, 0.89 for HF, and 0.95 for MP2. These scale factors were chosen so that the calculated vibrational wavenumbers for the most stable conformer of ME and MTE fit best with the experimental wavenumbers, and are actually close to
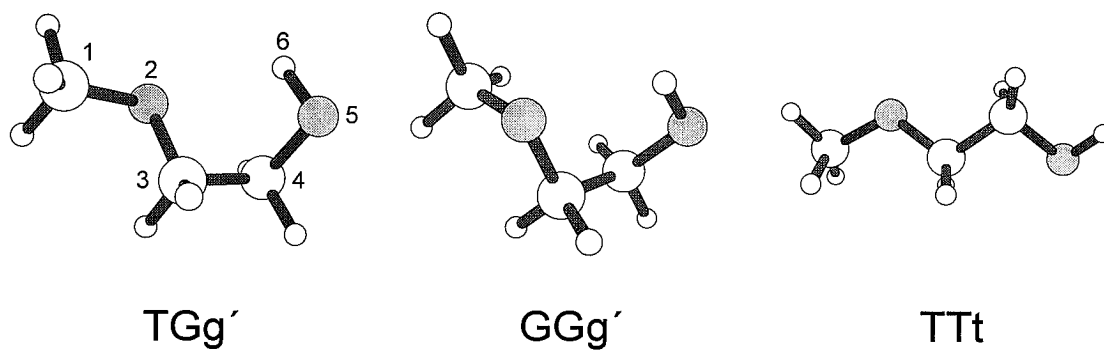
Figure 3.1   Structures of the most stable three conformers of 2-methoxyethanol (ME).
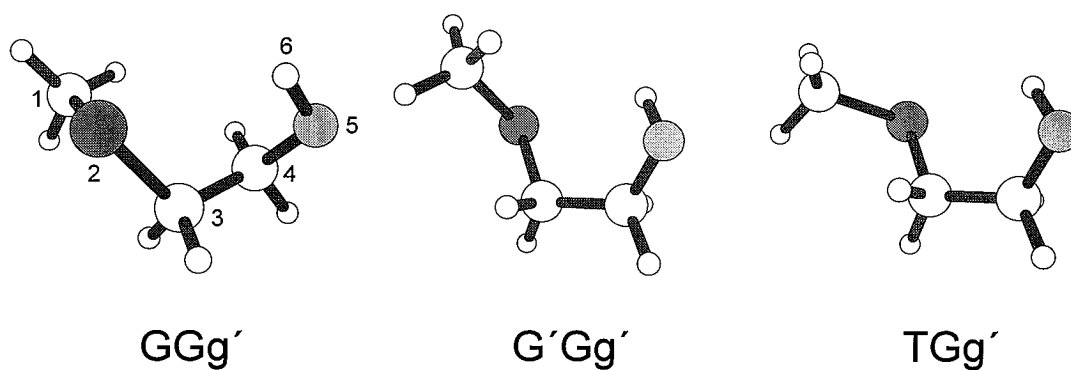
Figure 3.2   Structures of the most stable three conformers of 2-(methylthio)ethanol (MTE).

the scale factors derived from a large number of experimental wavenumbers.[20]

3.3 Results and Discussion

3.3.1 Energies of Conformers

Tables 3.1 and 3.2 give the energies calculated by various DFT methods (BLYP, B3LYP and B3PW91) and ab initio MO methods (HF and MP2) for the most stable three conformers and an additional conformer without intramolecular hydrogen bonding of ME (TGg′, GGg′, TTt, and TGt) and those of MTE (GGg′, G′Gg′, TGg′, and GGt). It should be remembered that the TGg′, GGg′, and G′Gg′ conformers can form intramolecular hydrogen bonding between the hydroxyl hydrogen atom and the ether oxygen or sulfur atom.

For ME, all of the calculations including electron correlation, namely MP2, BLYP, B3LYP, and B3PW91, predict the energies for the TGg′ and GGg′ conformers to be lower than the energy for the third most stable conformer TTt by 13.4–14.6 and 7.1–9.0 kJ mol^{-1}, respectively. The uncorrelated HF calculations give, on the other hand, the energy for the GGg′ conformer similar to the energy for the TTt conformer. These results indicate that the inclusion of electron correlation is important for predicting the conformational stabilization by intramolecular hydrogen bonding. The theoretical prediction in this work is consistent with the experimental findings by microwave spectroscopy[28] and matrix-isolation infrared spectroscopy[16] that only the TGg′ conformer is present in the gas phase and a low-temperature matrix.

The calculations on MTE by the MP2, BLYP, B3LYP, and B3PW91 methods show that the energies for the G′Gg′ and TGg′ conformers are higher than the energy for the most stable conformer GGg′ by 1.6–2.8 and 4.3 kJ mol^{-1}, respectively, while the calculations by the HF method show the energies for the G′Gg′ and TGg′ conformers to be similar to each other and higher than the energy for the GGg′ conformer by 2.5 kJ mol^{-1}. These results again suggest the importance of electron correlation in the calculations. Recent matrix-isolation infrared study has shown that the molecular conformations of MTE in a low-

56

Table 3.1 Relative Energies for the Most Stable Three Conformers and an Additional Conformer without Intramolecular Hydrogen Bonding of 2-Methoxyethanol Calculated by Various Methods[a]

conformer	relative energy/kJ mol^{-1}				
	HF	MP2	BLYP	B3LYP	B3PW91
TGg′	0.000	0.000	0.000	0.000	0.000
GGg′	8.874	6.269	5.512	6.300	6.163
TTt	8.604	14.584	14.484	13.404	13.377
TGt[b]	15.061	18.001	16.224	16.362	16.431

[a] The 6-31G* basis set was used. [b] The stabilization energy by intramolecular hydrogen bonding may be estimated as a difference of energies between the TGt and TGg′ conformers.

Table 3.2 Relative Energies for the Most Stable Three Conformers and an Additional Conformer without Intramolecular Hydrogen Bonding of 2-(Methylthio)ethanol Calculated by Various Methods[a]

conformer	relative energy/kJ mol^{-1}				
	HF	MP2[b]	BLYP	B3LYP	B3PW91
GGg′	0.000	0.000	0.000	0.000	0.000
G′Gg′	2.324	1.569	1.946	2.196	2.813
TGg′	2.825	4.377	4.325	4.267	4.302
GGt[c]	12.441	15.354	16.109	15.668	16.498

[a] The 6-31G* basis set was used. [b] Ref. 15. [c] The stabilization energy by intramolecular hydrogen bonding may be estimated as a difference of energies between the GGt and GGg′ conformers.

Table 3.3 Structural Parameters for the TGg′ Conformer of 2-Methoxyethanol Calculated by Various Methods[a] and Experimental Values

structural parameter	calculated					experimental[b]
	HF	MP2	BLYP	B3LYP	B3PW91	
Bond Lengths/Å						
C_1–O_2	1.3938	1.4195	1.4287	1.4125	1.4067	1.41
O_2–C_3	1.3989	1.4240	1.4382	1.4201	1.4144	1.41
C_3–C_4	1.5141	1.5130	1.5320	1.5209	1.5168	1.52
C_4–O_5	1.3975	1.4213	1.4336	1.4169	1.4109	1.41
O_5–H_6	0.9486	0.9741	0.9831	0.9719	0.9700	1.01
Bond Angles/deg						
C_1–O_2–C_3	114.64	112.08	113.03	113.38	113.06	111.7
O_2–C_3–C_4	107.27	105.77	106.34	106.58	106.54	109.5
C_3–C_4–O_5	111.37	110.43	111.32	111.20	111.14	112
C_4–O_5–H_6	107.74	104.68	104.40	105.27	105.14	105
Torsion Angles/deg						
C_1–O_2–C_3–C_4	−175.90	−173.36	−173.21	−173.79	−173.69	−172
O_2–C_3–C_4–O_5	60.60	59.74	60.26	59.74	59.48	57
C_3–C_4–O_5–H_6	−53.83	−50.17	−49.67	−49.94	−49.74	−45

[a] The 6-31G* basis set was used. [b] Microwave spectroscopy.[29] All of the bond lengths and bond angles were assumed in the structural analysis.

Table 3.4 Structural Parameters for the GGg′ Conformer of 2-(Methylthio)ethanol Calculated by Various Methods[a] and Experimental Values

structural parameter	calculated					experimental[b]
	HF	MP2[c]	BLYP	B3LYP	B3PW91	
Bond Lengths/Å						
C_1–S_2	1.8114	1.8099	1.8509	1.8293	1.8172	1.802
S_2–C_3	1.8198	1.8163	1.8635	1.8402	1.8275	1.806
C_3–C_4	1.5253	1.5241	1.5424	1.5313	1.5270	1.524
C_4–O_5	1.3952	1.4189	1.4290	1.4131	1.4065	1.415
O_5–H_6	0.9489	0.9753	0.9858	0.9737	0.9723	0.950
Bond Angles/deg						
C_1–S_2–C_3	101.42	99.83	100.88	100.86	100.92	100.2
S_2–C_3–C_4	114.21	113.03	113.15	113.30	113.13	114.7
C_3–C_4–O_5	112.54	111.94	112.56	112.53	112.47	112.5
C_4–O_5–H_6	109.00	106.12	105.34	106.32	106.14	104.0
Torsion Angles/deg						
C_1–S_2–C_3–C_4	77.04	75.09	76.30	75.58	75.16	67
S_2–C_3–C_4–O_5	62.38	61.04	58.82	59.56	58.86	61
C_3–C_4–O_5–H_6	−59.06	−55.57	−53.94	−53.76	−52.77	

[a] The 6-31G* basis set was used. [b] Microwave spectroscopy.[30] All of the bond lengths and bond angles were assumed in the structural analysis. [c] Ref. 15.

temperature matrix are GGg′ and G′Gg′, the former being more stable.[15] This experimental observation agrees with the results of the present higher-level calculations that only these two conformers lie within the lowest 2.8 kJ mol^{-1} energies.

The stabilization energies by the formation of intramolecular hydrogen bondings OH⋯O and OH⋯S are examined on the basis of the energies of the TGt conformer relative to the TGg′ conformer for ME and of the GGt conformer relative to the GGg′ conformer for MTE (Tables 3.1 and 3.2). The HF and MP2 calculations give the stabilization energy by OH⋯S hydrogen bonding significantly smaller than the energy by OH⋯O hydrogen bonding. The DFT calculations give, on the other hand, the stabilization energy of 15.7–16.5 kJ mol^{-1} for OH⋯S hydrogen bonding, which is substantially the same as that for OH⋯O hydrogen bonding.

3.3.2 Molecular Geometries

The calculated structural parameters for the TGg′ conformer of ME and the GGg′ conformer of MTE are given in Table 3.3 and Table 3.4, respectively, where the experimental values by microwave spectroscopy[28,29] are also included. The overall agreement between the calculated and experimental results is satisfactory. It is noted that the BLYP method gives the bond lengths for the two compounds always longer, while the HF method gives these generally shorter, than those obtained by other methods. In the HF calculations, the C–O and O–H bond lengths, in particular, are significantly shorter than in other calculations. The bond angles calculated by the three DFT methods are almost coincident with one another, but are slightly different from those calculated by the HF and MP2 methods.

3.3.3 Vibrational Wavenumbers

The vibrational wavenumbers for the most stable conformer of ME and MTE, namely TGg′ for the former and GGg′ for the latter, are given in Tables 3.5 and

3.6, respectively, where the calculated wavenumbers have been corrected with uniform scale factors for the respective methods and the experimental wavenumbers are taken from the studies of matrix-isolation infrared spectroscopy.[15,16] Graphical representations of the wavenumbers and intensities for these conformers are displayed in Figures 3.3 and 3.4. These figures show that the calculated results by the MP2, B3LYP, and B3PW91 methods are in good agreement with the experimental data. The BLYP method gives the C–O stretching wavenumbers, 1095 and 1034 cm^{-1} for ME and 1038 cm^{-1} for MTE, which are significantly lower than the experimental wavenumbers, 1133 and 1066 cm^{-1} for ME and 1072 cm^{-1} for MTE. The BLYP calculations also give a notably low C–S stretching wavenumber 604 cm^{-1} in comparison with the experimental wavenumber 656 cm^{-1}. These low wavenumbers for the C–O and C–S stretching vibrations are obviously related to the overestimated lengths of the relevant bonds.

The calculated and experimental O–H stretching wavenumbers for the TGg′ conformer of ME and the GGg′ conformer of MTE are given in Table 3.7. It is clear for these conformers that intramolecular hydrogen bonding is formed between the hydroxyl hydrogen atom and the ether oxygen or sulfur atom. The previous matrix-isolation infrared studies have shown that the intramolecular hydrogen bonded O–H stretching wavenumber for MTE (3537 cm^{-1}) is considerably lower than that for ME (3625 cm^{-1}) with a difference of 88 cm^{-1}.[15,16] The HF calculations give this wavenumber difference to be only 10 cm^{-1}, while the MP2 calculations give this to be 27 cm^{-1}. The DFT calculations, on the other hand, show larger wavenumber differences of 41–57 cm^{-1}, in much better agreement with the experimental observation. The difference in the calculated O–H stretching wavenumbers between ME and MTE reflects the difference in the O–H bond lengths (Table 3.3 and Table 3.4). The HF calculations give the bond lengths for the two compounds to be essentially the same (0.9486 and 0.9489 Å), while the three DFT calculations give the O–H bond length for ME shorter than that for MTE by about 0.002 Å. These results suggest that electron correlation is important for predicting the geometries and wavenumbers for molecules with intramolecular hydrogen bonding.

Table 3.5 Calculated and Experimental Vibrational Wavenumbers[a] for the TGg′ Conformer of 2-Methoxyethanol

ν_{calc}/cm^{-1}[b]					ν_{exp}/cm^{-1}[c]	vibrational assignment[d]
HF[e]	MP2[f]	BLYP[g]	B3LYP[h]	B3PW91[i]		
1490	1502	1509	1503	1500	1479	CH_2 scissor
1477	1489	1489	1485	1481	1474	CH_2 scissor
1472	1486	1487	1483	1478	1462	CH_3 asymmetric deformation
1464	1475	1473	1470	1467	1459	CH_3 asymmetric deformation
1455	1451	1459	1457	1453	1449	CH_3 symmetric deformation
1420	1407	1416	1416	1415	1406	CH_2 wag
1380	1366	1378	1378	1374	1370	CH_2 wag
1348	1349	1362	1360	1358	1348	CH_2 wag, C–O–H bend
1244	1235	1239	1242	1243	1244	CH_3 rock, CH_2 twist
1231	1220	1223	1228	1231	1233	CH_2 twist
1177	1166	1168	1173	1176	1179	CH_2 twist, CH_3 rock
1157	1152	1157	1160	1160	1165	CH_3 rock
1143	1129	1095	1134	1151	1133	CH_3–O stretch, C–O(CH_3) stretch
1105	1105	1105	1107	1111	1109	CH_2 rock
1068	1061	1034	1059	1071	1066	C–O(H) stretch, C–C stretch

(Continued)

1005	998	986	1003	1014	1014	CH_2 rock, C–O(CH_3) stretch
882	894	879	889	895	895	C–O(H) stretch, CH_2 rock
824	826	815	826	832	837	C–O(CH_3) stretch, CH_2 rock
525	535	534	536	537		C–C–O(H) bend, C–C–O(CH_3) bend
400	443	451	443	442		C–O(H) torsion
352	366	363	363	362		CH_3–O–C bend, C–C–O(H) bend
263	273	272	272	271		C–C–O(CH_3) bend, CH_3–O–C bend
214	230	232	228	228		CH_3–O torsion
140	152	145	145	143		C–C torsion
88	89	95	95	95		C–O(CH_3) torsion

[a] Wavenumbers higher than 1600 cm^{-1} are not given in this Table. [b] The 6-31G* basis set was used. [c] Matrix-isolation infrared spectroscopy.[16] [d] Ref. 16. [e] Scaled by a uniform factor of 0.89. [f] Scaled by a uniform factor of 0.95. [g] Scaled by a uniform factor of 1.00. [h] Scaled by a uniform factor of 0.97. [i] Scaled by a uniform factor of 0.97.

Table 3.6 Calculated and Experimental Vibrational Wavenumbers[a] for the GGg′ Conformer of 2-(Methylthio)ethanol

ν_{calc}/cm^{-1b}					ν_{exp}/cm^{-1c}	vibrational assignment[d]
HF[e]	MP2[d,f]	BLYP[g]	B3LYP[h]	B3PW91[i]		
1483	1496	1496	1493	1491	1482	CH_2 scissor
1453	1471	1476	1468	1463	1443	CH_3 asymmetric deformation
1441	1454	1462	1454	1449	1430	CH_3 asymmetric deformation
1424	1433	1439	1435	1428	1412	CH_2 scissor
1396	1387	1401	1398	1397	1390	CH_2 wag
1354	1369	1361	1359	1357	1341	C–O–H bend, CH_2 wag
1348	1348	1345	1348	1347	1332	CH_3 symmetric deformation
1298	1299	1285	1290	1288	1278	CH_2 wag
1198	1201	1192	1197	1200	1195	CH_2 twist
1155	1162	1166	1168	1172	1177	CH_2 twist
1083	1070	1038	1069	1088	1072	C–O stretch, C–C stretch
1040	1055	1045	1047	1048	1047	CH_3 rock, CH_2 rock
959	979	957	959	961	957	CH_3 rock
947	961	945	948	948	948	CH_3 rock, CH_2 rock
910	929	899	911	919	929	C–C stretch, CH_2 rock

(Continued)

808	820	811	815	816		CH_2 rock, C–O stretch
707	734	671	696	717		CH_3–S stretch
629	659	604	624	641	656	C–S stretch
460	469	470	471	473		C–C–O bend, C–C–S bend
384	420	439	426	430		C–O torsion
309	323	315	317	317		C–S–C bend, C–C–S bend
212	222	211	213	214		C–S–C bend, C–C–S bend
170	181	159	165	171		C–C torsion, CH_3–S torsion
136	141	132	132	131		CH_3–S torsion, C–C torsion
68	68	73	71	72		C–S torsion

66

[a] Wavenumbers higher than 1600 cm^{-1} are not given in this Table. [b] The 6-31G* basis set was used. [c] Matrix-isolation infrared spectroscopy.[15] [d] Ref. 15. [e] Scaled by a uniform factor of 0.89. [f] Scaled by a uniform factor of 0.95. [g] Scaled by a uniform factor of 1.00. [h] Scaled by a uniform factor of 0.97. [i] Scaled by a uniform factor of 0.97.
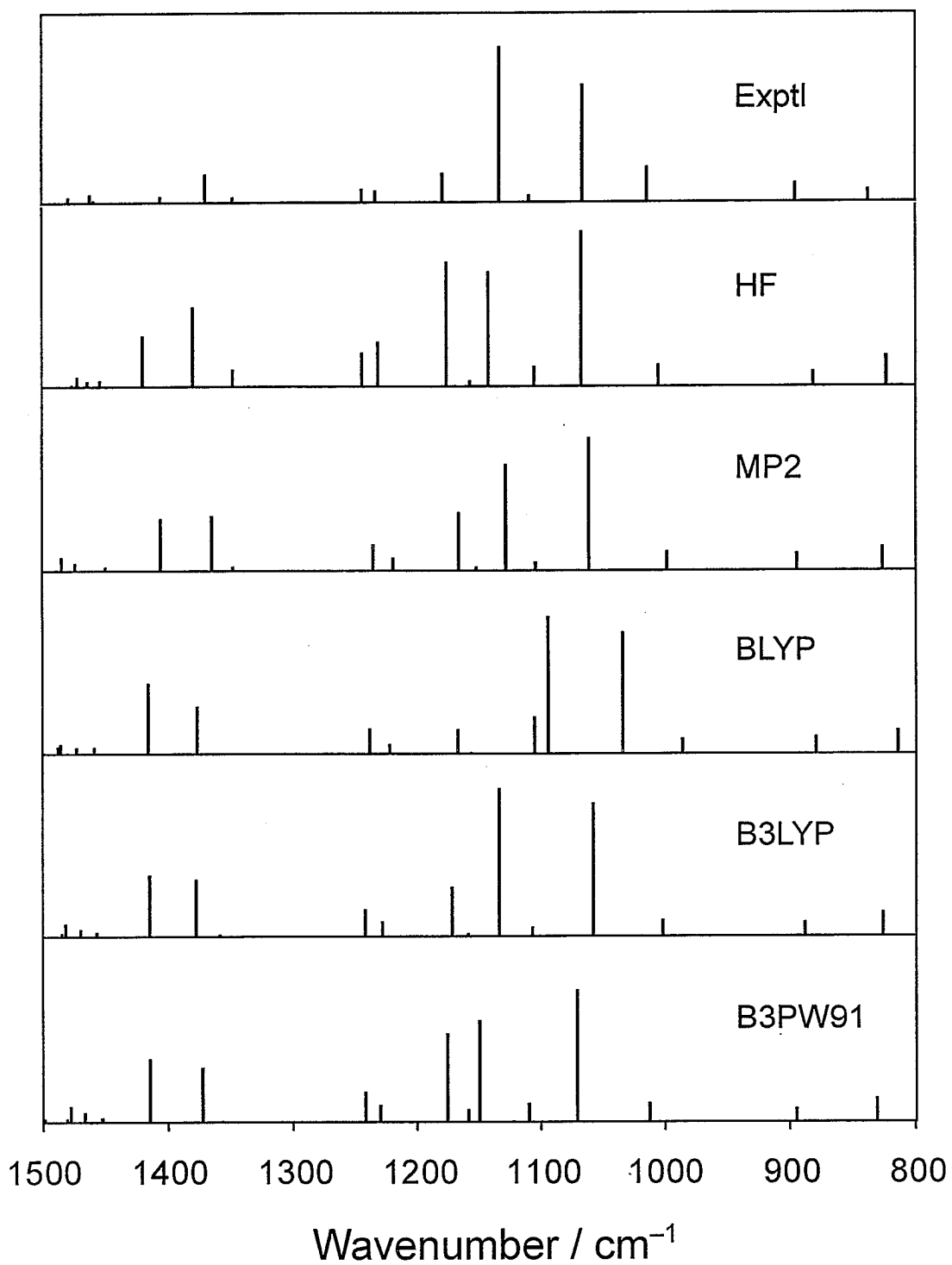
Figure 3.3 Experimental and calculated wavenumbers and intensities for the TGg' conformer of 2-methoxyethanol (ME).
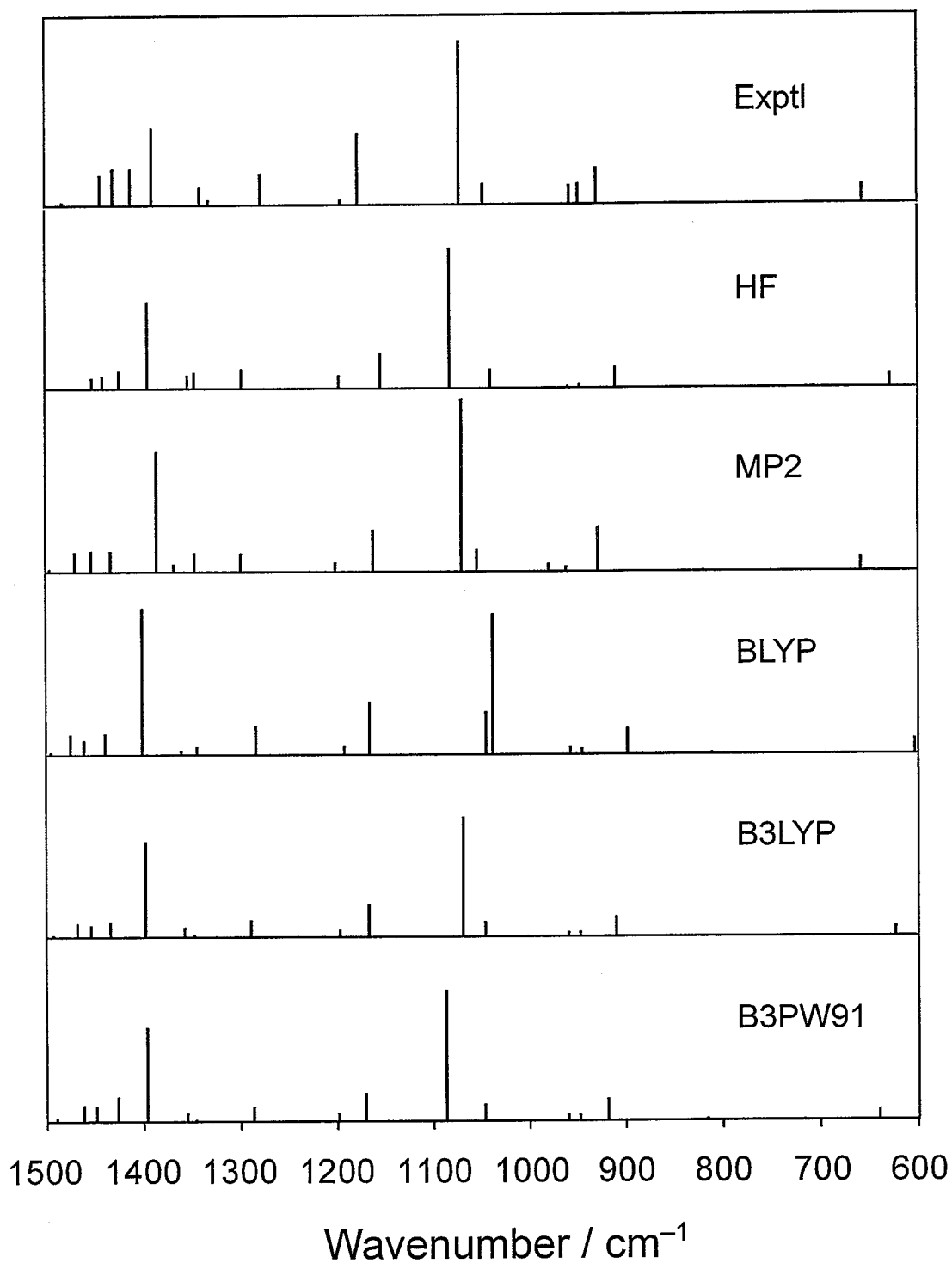
Figure 3.4 Experimental and calculated wavenumbers and intensities for the GGg′ conformer of 2-(methylthio)ethanol (MTE).

Table 3.7 Calculated and Experimental O–H Stretching Wavenumbers for the TGg′ Conformer of 2-Methoxyethanol (ME) and the GGg′ Conformer of 2-(Methylthio)ethanol (MTE)

compound	ν_{calc}/cm^{-1a}					ν_{exp}/cm^{-1b}
	HF[c]	MP2[d]	BLYP[e]	B3LYP[f]	B3PW91[g]	
ME (TGg′)	3646	3564	3559	3610	3645	3625[h]
MTE (GGg′)	3636	3537[i]	3502	3569	3593	3537
$\nu_{ME} - \nu_{MTE}$	10	27	57	41	52	88

[a] The 6-31G* basis set was used. [b] Matrix-isolation infrared spectroscopy.[15,16] [c] Scaled by a uniform factor of 0.89. [d] Scaled by a uniform factor of 0.95. [e] Scaled by a uniform factor of 1.00. [f] Scaled by a uniform factor of 0.97. [g] Scaled by a uniform factor of 0.97. [h] Averaged wavenumber of 3630 and 3620 cm^{-1}. [i] Ref. 15.

Recent studies on the evaluation of various DFT methods have indicated that Becke's three-parameter hybrid functional methods are the most successful among others for predicting molecular geometries and vibrational wavenumbers for a variety of organic compounds.[19,20,30] The present study on ME and MTE has confirmed the excellent performance of the B3PW91 and B3LYP calculations as discussed above.

3.4 Conclusions

The energies, molecular geometries, and vibrational wavenumbers for several important conformers of ME and MTE have been calculated by the HF, MP2, BLYP, B3LYP, and B3PW91 methods using the 6-31G* basis set. The calculated energies are consistent with the experimental findings that the TGg' conformer of ME and the GGg' and G'Gg' conformers of MTE are present in a low-temperature matrix. The DFT calculations give the stabilization energy by OH⋯S hydrogen bonding substantially the same as the energy by OH⋯O hydrogen bonding. The vibrational wavenumbers for the TGg' conformer of ME and the GGg' conformer of MTE are successfully predicted by the MP2, B3LYP, and B3PW91 methods using uniform scale factors for the respective methods. The experimental large wavenumber difference between ME and MTE of the intramolecular hydrogen bonded O–H stretching vibrations is reproduced much better with the DFT calculations than with the ab initio MO calculations. This study has shown that Becke's three-parameter hybrid functional methods overall give the most accurate results.

References

(1) Mizushima, S. *Structure of Molecules and Internal Rotation*; Academic Press: New York, 1954.

(2) Joesten, M. D.; Schaad, L. J. *Hydrogen Bonding*; Marcel Dekker: New York, 1974.

(3) Schuster, P.; Zundel G.; Sandorfy, C., Eds.; *The Hydrogen Bond*; North-Holland: Amsterdam, 1976; Vols 1, 2 and 3.

(4) Astrup, E. E. *Acta Chem. Scand.* **1979**, *A33*, 655–664.

(5) Yoshida, H.; Kaneko, I.; Matsuura, H.; Ogawa, Y.; Tasumi, M. *Chem. Phys. Lett.* **1992**, *196*, 601–606.

(6) Yoshida, H.; Tanaka, T.; Matsuura, H. *Chem. Lett.* **1996**, 637–638.

(7) Tsuzuki, S.; Uchimaru, T.; Tanabe, K.; Hirano, T. *J. Phys. Chem.* **1993**, *97*, 1346–1350.

(8) Jaffe, R. L.; Smith, G. D.; Yoon, D. Y. *J. Phys. Chem.* **1993**, *97*, 12745–12751.

(9) Smith, G. D.; Jaffe, R. L.; Yoon, D. Y. *J. Phys. Chem.* **1993**, *97*, 12752–12759.

(10) Müller-Plathe, F.; van Gunsteren, W. F. *Macromolecules* **1994**, *27*, 6040–6045.

(11) Smith, G. D.; Jaffe, R. L.; Yoon, D. Y. *J. Am. Chem. Soc.* **1995**, *117*, 530–531.

(12) Liu, H.; Müller-Plathe, F.; van Gunsteren, W. F. *J. Chem. Phys.* **1995**, *102*, 1722–1730.

(13) Williams, D. J.; Hall, K. B. *J. Phys. Chem.* **1996**, *100*, 8224–8229.

(14) Taylor, R.; Kennard, O. *J. Am. Chem. Soc.* **1982**, *104*, 5063–5070.

(15) Chapter 2 of this thesis. Yoshida, H.; Harada, T.; Murase, T.; Ohno, K.; Matsuura, H. *J. Phys. Chem. A* **1997**, *101*, 1731–1737.

(16) Yoshida, H.; Takikawa, K.; Ohno, K.; Matsuura, H. *J. Mol. Struct.* **1993**, *299*, 141–147.

(17) Parr, R. G.; Yang, W. *Density-Functional Theory of Atoms and Molecules*; Oxford University Press: New York, 1989.

(18) Johnson, B. G.; Gill, P. M. W.; Pople, J. A. *J. Chem. Phys.* **1993**, *98*, 5612–5626.

(19) Rauhut, G.; Pulay, P. *J. Phys. Chem.* **1995**, *99*, 3093–3100.

(20) Scott, A. P.; Radom, L. *J. Phys. Chem.* **1996**, *100*, 16502–16513.

(21) Becke, A. D. *Phys. Rev. A* **1988**, *38*, 3098–3100.

(22) Lee, C.; Yang, W.; Parr, R. G. *Phys. Rev. B* **1988**, *37*, 785–789.

(23) Becke, A. D. *J. Chem. Phys.* **1993**, *98*, 5648–5652.

(24) Perdew, J. P. In *Electronic Structure of Solids '91*; Ziesche, P., Eschrig, H., Eds.; Akademie Verlag: Berlin, 1991.

(25) Perdew, J. P.; Wang, Y. *Phys. Rev. B* **1992**, *45*, 13244–13249.

(26) Perdew, J. P.; Chevary, J. A.; Vosko, S. H.; Jackson, K. A.; Pederson, M. R.; Singh, D. J.; Fiolhais, C. *Phys. Rev. B* **1992**, *46*, 6671–6687.

(27) Frisch, M. J.; Trucks, G. W.; Schlegel, H. B.; Gill, P. M. W.; Johnson, B. G.; Robb, M. A.; Cheeseman, J. R.; Keith, T.; Petersson, G. A.; Montgomery, J. A.; Raghavachari, K.; Al-Laham, M. A.; Zakrzewski, V. G.; Ortiz, J. V.; Foresman, J. B.; Cioslowski, J.; Stefanov, B. B.; Nanayakkara, A.; Challacombe, M.; Peng, C. Y.; Ayala, P. Y.; Chen, W.; Wong, M. W.; Andres, J. L.; Replogle, E. S.; Gomperts, R.; Martin, R. L.; Fox, D. J.; Binkley, J. S.; Defrees, D. J.; Baker, J.; Stewart, J. P.; Head-Gordon, M.; Gonzalez, C.; Pople, J. A. *Gaussian 94*, Revision D.3; Gaussian Inc., Pittsburgh, PA, 1995.

(28) Buckley, P.; Brochu, M. *Can. J. Chem.* **1972**, *50*, 1149–1156.

(29) Marstokk, K.-M.; Møllendal, H.; Uggerud, E. *Acta Chem. Scand.* **1989**, *43*, 26–31.

(30) El-Azhary, A. A.; Suter, H. U. *J. Phys. Chem.* **1996**, *100*, 15056–15063.

Chapter 4

Matrix-Isolation Infrared Spectroscopic and Density Functional Studies on Intramolecular Hydrogen Bonding in $CH_3XCH_2CH_2OH$ (X = O, S, and Se)

Abstract

The conformational stability of 2-(methylseleno)ethanol has been studied by vibrational spectroscopy and density functional theory. In an argon matrix, the molecules assume primarily the gauche$^{\pm}$–gauche$^{\pm}$–gauche$^{\mp}$ (GGg′) and gauche$^{\mp}$–gauche$^{\pm}$–gauche$^{\mp}$ (G′Gg′) conformations around the CH_3Se–CH_2–CH_2–OH bonds, being consistent with the theoretical energies of the conformers. The GGg′ and G′Gg′ conformers are stabilized by intramolecular OH···Se hydrogen bonding. The conformational stabilization energy by this hydrogen bonding was estimated by density functional calculations as 14.5 kJ mol^{-1}, which is substantially the same as the corresponding energies for OH···O and OH···S hydrogen bonding. These experimental and theoretical results show that intramolecular OH···Se hydrogen bonding is as strong as OH···O and OH···S hydrogen bonding. An additional intramolecular CH···O interaction with its stabilization energy 5.6 kJ mol^{-1} stabilizes the G′G conformation around the CH_3Se–CH_2–CH_2OH bonds. The spectral observation that the wavenumbers of the hydrogen-bonded O–H stretching mode for 2-(methylseleno)ethanol and the thio-analogue are significantly lower than the wavenumber for the oxy-analogue was also discussed.

4.1 Introduction

The conformation of molecules is important in molecular sciences, in particular, in relation to the emergence of relevant functions of the molecular system. It has been established that, among a number of factors, intramolecular and intermolecular interactions play an important role in determining the conformation of the molecule. Hydrogen bonding has long been known as one of the crucial interactions that stabilize particular conformations of many organic and biological molecules.[1] Recent studies have shown that new types of hydrogen-involved weaker interactions play an important role in the conformational stabilization of molecules.[2-6]

To elucidate conformational implications of intramolecular hydrogen bonding, the conformations of 2-methoxyethanol, $CH_3OCH_2CH_2OH$,[7] and 2-(methylthio)ethanol, $CH_3SCH_2CH_2OH$,[8] have been studied by matrix-isolation infrared spectroscopy. These studies have shown that the molecules in the matrix-isolated state assume only the conformations stabilized by intramolecular hydrogen bonding, OH···O or OH···S. It was also shown on the basis of density functional calculations that the conformational stabilization energy by the formation of OH···S hydrogen bonding is substantially the same as the corresponding energy by the formation of OH···O hydrogen bonding.[9] The results of these previous studies indicate that intramolecular hydrogen bonding is strong enough to be a dominant factor determining the molecular conformation in the isolated state.

In addition to the generally accepted intramolecular hydrogen bonding such as OH···O or OH···S, a new type of intramolecular attractive interaction between a hydrogen atom in the methyl or methylene group and an oxygen atom, i.e., CH···O interaction, has now been well recognized as an important interaction that determines the molecular conformation.[2-5] This interaction was experimentally evidenced for the relevant conformers of 1,2-dimethoxyethane, $CH_3OCH_2CH_2OCH_3$,[2] and 1-methoxy-2-(methylthio)ethane, $CH_3OCH_2CH_2SCH_3$,[5] in the matrix-isolated state. The same interaction deserves considering in the conformational stabilization of 2-methoxyethanol and 2-

75

(methylthio)ethanol. The previous studies on these compounds have in fact shown that intramolecular CH···O interaction competes with OH···O or OH···S hydrogen bonding in determining the conformation.[7,8] A distinctive property of this attractive interaction is the shortening of the relevant C–H bond,[8,10–14] being different from the lengthening of the O–H bond on the formation of OH···O or OH···S hydrogen bonding.

To gain a further insight into the implications of possible intramolecular interactions in the conformational stabilization of a series of $CH_3XCH_2CH_2OH$ compounds, the conformation of 2-(methylseleno)ethanol, $CH_3SeCH_2CH_2OH$, a compound that contains a heteroatom X of a higher-periodic element selenium, have been investigated by matrix-isolation infrared spectroscopy and density functional theory. The Raman spectra of this compound in the liquid and solid states were also studied for comparison of the conformational relevance of intramolecular and intermolecular interactions in different phases.

4.2 Experimental Section

2-(Methylseleno)ethanol was kindly supplied by Professor Shuji Tomoda, the University of Tokyo. For reference, the method of synthesis of this compound is described below. 2-(Methylseleno)ethanol was prepared by reacting bis(2-hydroxyethyl) diselenide with sodium tetrahydroborate and then with dimethyl sulfate in absolute ethanol under nitrogen atmosphere at 0 °C.[15] Bis(2-hydroxyethyl) diselenide was prepared by treating the mixture of powdered sodium hydroxide, selenium, and *N,N*-dimethylformamide with hydrazine hydrate and then with 2-bromoethanol.[16,17] The crude products of bis(2-hydroxyethyl) diselenide and 2-(methylseleno)ethanol were purified by column chromatography on silica gel (hexane/ethyl acetate = 4/1).

The infrared spectra of 2-(methylseleno)ethanol in an argon matrix were measured with a JASCO FT/IR-350 Fourier transform spectrometer using a deuterated triglycine sulfate (DTGS) detector. Premixed gas of Ar/2-(methylseleno)ethanol = 2000 was slowly sprayed and deposited onto a cesium iodide plate cooled to 11 K by an Iwatani CryoMini D105 refrigerator. The

spectra were obtained by coaddition of 100 scans at a resolution of 1 cm^{-1}. To study the spectral changes with increasing temperature, the deposited sample was annealed at different temperatures up to 41 K and was subsequently cooled back to 11 K to measure the spectra. The Raman spectra in the liquid state at various temperatures and in the solid state at 77 K were recorded on a JASCO NR-1800 Raman spectrometer equipped with a Princeton Instruments CCD detector. An NEC argon ion laser GLG 2162 operating at 514.5 nm was used for excitation.

4.3 Calculations

The density functional calculations of the energies, structural parameters, and vibrational wavenumbers for 12 optimized conformers of 2-(methylseleno)ethanol were performed by using Becke's three-parameter hybrid functional[18] combined with the Lee–Yang–Parr correlation functional[19] (B3LYP). The basis set used was 6-311+G**. The optimized structures of the 12 conformers are depicted in Figure 4.1. The calculation failed the optimization of geometries for the TGg' and GGg conformers. The density functional calculations were carried out with the Gaussian 98 program.[20] The input data for the Gaussian 98 program were prepared by using the graphical molecular modeling program Molda.[21] The calculated vibrational wavenumbers were scaled by the wavenumber-linear scaling (WLS) method using a relationship proposed previously.[22] The B3LYP/6-311+G** calculations were also performed on several selected conformers of 2-methoxyethanol and 2-(methylthio)ethanol.

4.4 Results and Discussion

4.4.1 Energies of Conformers

The relative energies of 12 optimized conformers of 2-(methylseleno)ethanol (MSE) calculated by the B3LYP/6-311+G** method are given in Table 4.1, where the intramolecular interactions involved are indicated for the relevant
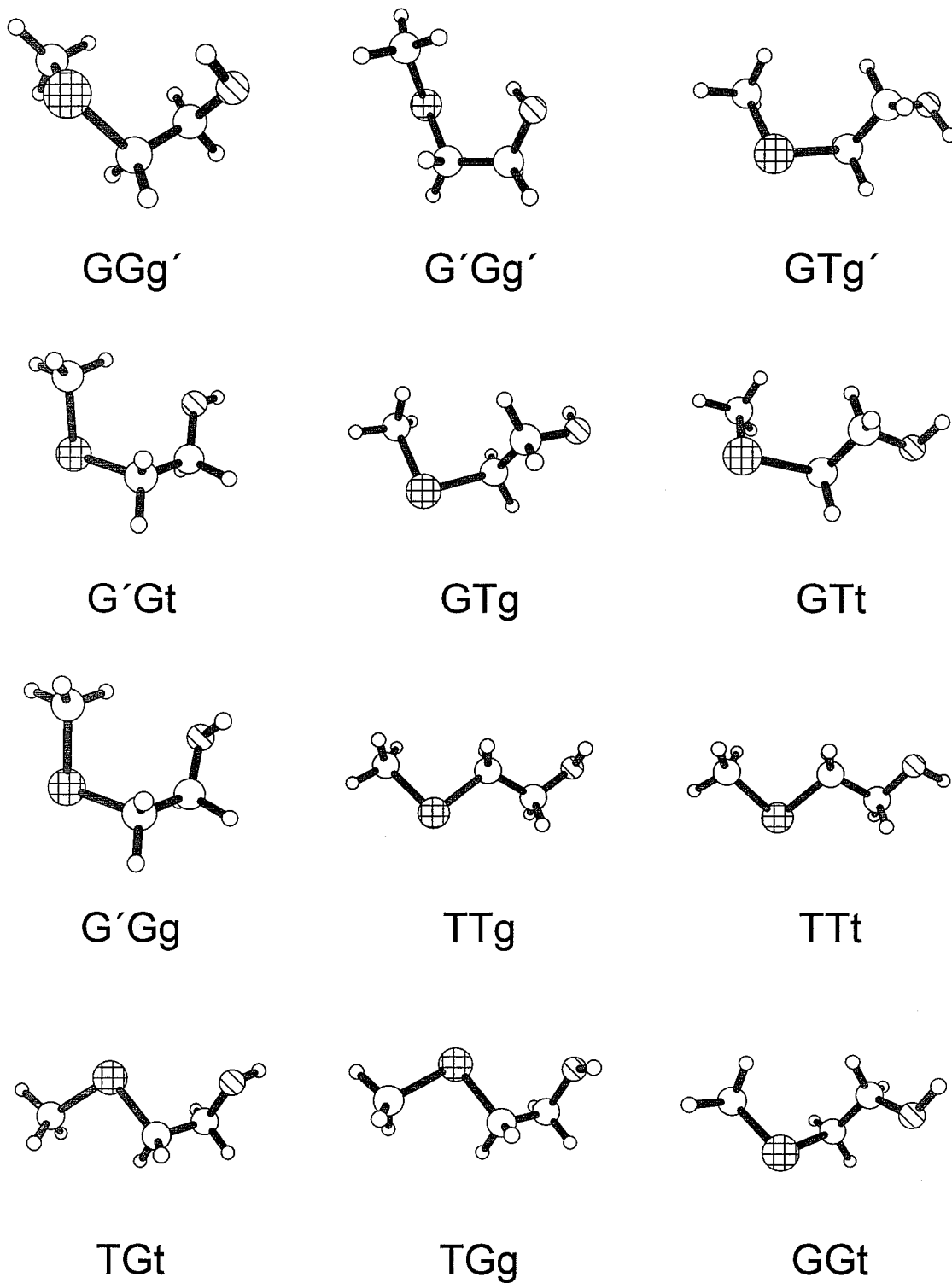
Figure 4.1 Optimized structures of 12 conformers of 2-(methylseleno)ethanol. Minimum-energy geometries for the TGg′ and GGg conformers were not attained. The atoms shown hatched are oxygen and the atoms shown crosshatched are selenium.

78

Table 4.1 Relative Energies of Conformers of 2-(Methylseleno)ethanol Calculated by the B3LYP/6-311+G** Method

conformer	relative energy^a/kJ mol^{-1}	interaction involved^b
GGg′	0.000	OH···Se
G′Gg′	3.169	OH···Se, CH···O
GTg′	6.834	
G′Gt	7.657	CH···O
GTg	7.691	
GTt	7.924	
G′Gg	10.691	CH···O
TTg	10.710	
TTt	11.369	
TGt	12.266	
TGg	12.353	
GGt	13.288	
TGg′	—^{c}	
GGg	—^{c}	

^{a} Relative energy with respect to the energy of the GGg′ conformer. ^{b} OH···Se, intramolecular OH···Se hydrogen bonding; CH···O, intramolecular 1,5-CH···O interaction. ^{c} Minimum-energy geometry was not attained.
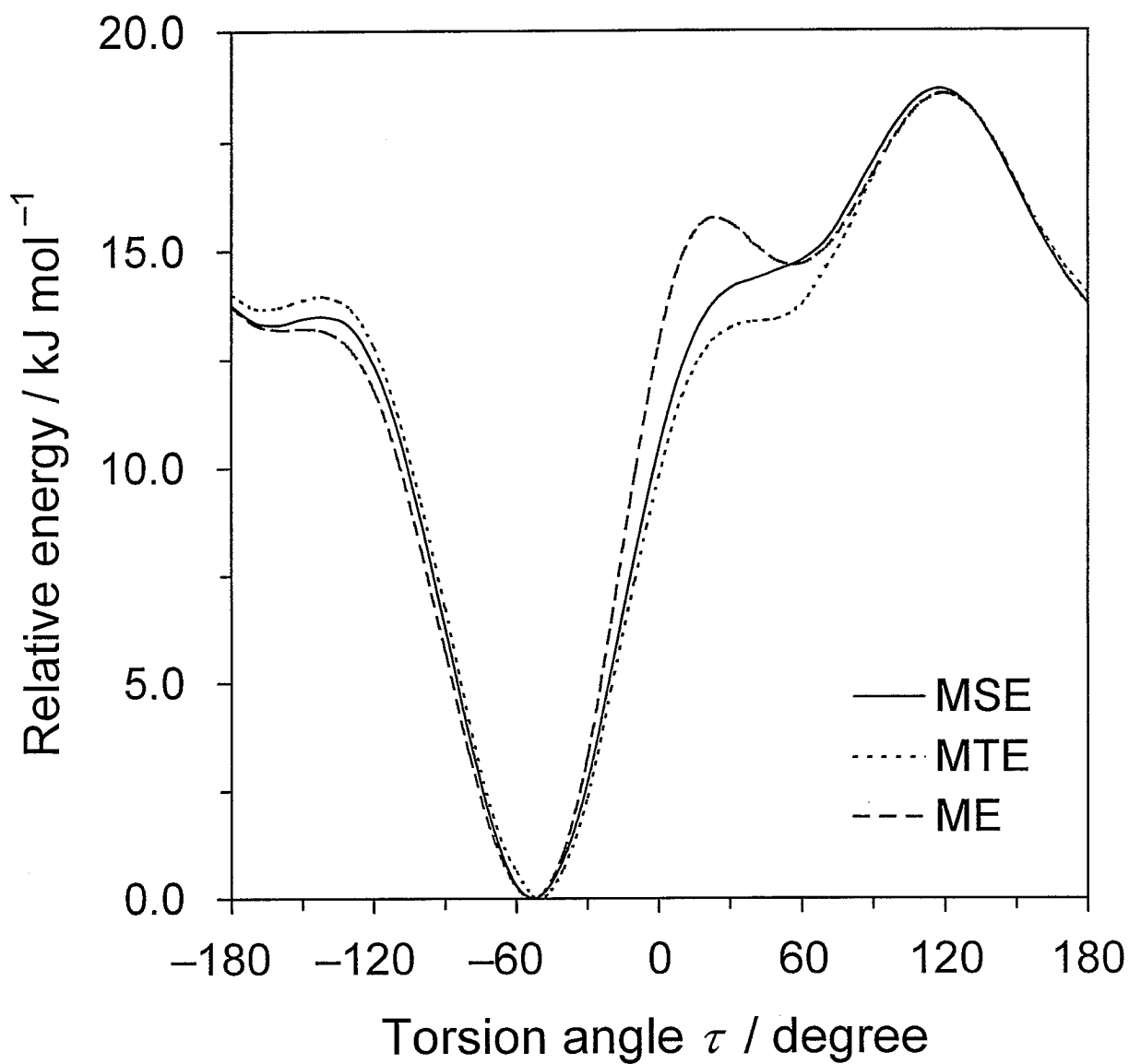
Figure 4.2 Energy curves for the GG[τ] conformation of 2-(methylseleno)ethanol (MSE), the GG[τ] conformation of 2-(methylthio)ethanol (MTE), and the TG[τ] conformation of 2-methoxyethanol (ME), with varying torsion angle τ around the CH_2CH_2–OH bond.

conformers. The molecular conformation of MSE is designated for a sequence of the three bonds $CH_3Se-CH_2-CH_2-OH$ by the symbols T or t for trans, G or g for gauche$^{\pm}$, and G′ or g′ for gauche$^{\mp}$, and the lower-case symbols apply to the conformation around the CH_2CH_2-OH bond.

The calculated results indicate that the most stable conformer of MSE is GGg′ and the second most stable conformer is G′Gg′ with an energy 3.2 kJ mol^{-1} higher than the energy of GGg′. These two conformers are stabilized by intramolecular hydrogen bonding between the hydroxyl hydrogen atom and the selenium atom (OH···Se). The conformational stabilization energy by OH···Se hydrogen bonding can be estimated as an energy difference between the non-hydrogen-bonded conformer GGg and the hydrogen-bonded conformer GGg′, as only the sign of the gauche for the CH_2CH_2-OH bond is different from each other in these conformers. Since the minimum-energy geometry of the GGg conformer was not attained, the energies of the GG[τ] conformation with varying torsion angle τ around the CH_2CH_2-OH bond were calculated. For each conformation with a fixed value of τ, the molecular geometry was optimized to yield the minimized energy. The energy curve thus obtained for the GG[τ] conformation is shown in Figure 4.2, where the energy curve for the GG[τ] conformation of 2-(methylthio)ethanol (MTE), for the which the GGg′ conformer is the most stable,[8,9] and the energy curve for the TG[τ] conformation of 2-methoxyethanol (ME), for which the TGg′ conformer is the most stable,[7,9] are also shown.

The energy curve for the GG[τ] conformation of MSE shows a deep minimum at $\tau = -54°$ corresponding to the most stable conformation GGg′ and a shallow hollow at $\tau \approx 50°$ corresponding to the unoptimized conformation GGg. The conformational stabilization energy by OH···Se hydrogen bonding is obtained as 14.5 kJ mol^{-1} as the difference of energies at $\tau \approx 50°$ (GGg) and $-54°$ (GGg′). The energy curves for MTE and ME give the conformational stabilization energies by OH···S and OH···O hydrogen bonding as 13.4 and 14.7 kJ mol^{-1}, respectively, as the energy difference between the GGg and GGg′ conformations for MTE and between the TGg and TGg′ conformations for ME. It is shown from these conformational stabilization energies that OH···Se

81

hydrogen bonding is as strong as OH$\cdots$O or OH$\cdots$S hydrogen bonding. This remarkable finding is manifested by the spectral observation, as described later, that MSE molecules in an argon matrix assume primarily the GGg$'$ and G$'$Gg$'$ conformations stabilized by OH$\cdots$Se hydrogen bonding.

It is important to note that the G$'$Gt conformer is more stable than the GGt conformer by 5.6 kJ mol^{-1}. In these conformers, the $CH_3Se-CH_2CH_2$ bond and the $SeCH_2-CH_2OH$ bond are in the gauche conformation, but the signs of the two gauche conformations are different in the G$'$Gt conformer and are the same for the GGt conformer, with the CH_2CH_2-OH bond in common in the trans conformation. Therefore, the stabilization energy for the G$'$Gt conformer, 5.6 kJ mol^{-1}, is considered to be associated with an interaction specific to the G$'$G conformation around the $CH_3Se-CH_2-CH_2OH$ bonds. The stabilization of the G$'$G conformation arises obviously from 1,5-CH$\cdots$O interaction, which has been evidenced for 1,2-dimethoxyethane[2] and 1-methoxy-2-(methylthio)ethane.[5] The stabilization of the G$'$G conformation around $CH_3S-CH_2-CH_2OH$ bonds in MTE has also been explained by this interaction.[8] A comparison of the stabilization energies of MSE by OH$\cdots$Se hydrogen bonding (14.5 kJ mol^{-1}) and CH$\cdots$O interaction (5.6 kJ mol^{-1}) indicates that the contribution of OH$\cdots$Se hydrogen bonding to the conformational stabilization is much larger than that of CH$\cdots$O interaction.

The results of calculations (Table 4.1) show that the gauche conformation is more stable than the trans conformation around the $CH_3Se-CH_2CH_2$ bond. This is the same propensity as found for the $CH_3S-CH_2CH_2$ bond of MTE.[8] The calculated results also show that for the $SeCH_2-CH_2OH$ bond the trans conformation is intrinsically more stable than the gauche conformation, but in cases where OH$\cdots$Se hydrogen bonding or CH$\cdots$O interaction is involved the conformation around this bond is impelled to assume the gauche conformation as described above. This conformational property of the $SeCH_2-CH_2OH$ bond is similar, more or less, to that of the SCH_2-CH_2OH and OCH_2-CH_2OH bonds.

Table 4.2 Bond Lengths and Nonbonded Interatomic Distances for Conformers of 2-(Methylseleno)ethanol

structural parameter	GGg'	G'Gg'	GTg'	G'Gt	GTg	GTt	G'Gg	TTg	TTt	TGt	TGg	GGt
					Bond Lengths[a]/Å							
O–H	0.9673	0.9668	0.9627	0.9616	0.9626	0.9621	0.9625	0.9627	0.9620	0.9615	0.9630	0.9610
C–H (CH$_3$)	1.0894	1.0881[b]	1.0894	1.0863[b]	1.0897	1.0894	1.0865[b]	1.0892	1.0893	1.0895	1.0896	1.0897
	1.0886	1.0889	1.0885	1.0893	1.0885	1.0886	1.0899	1.0893	1.0893	1.0898	1.0897	1.0896
	1.0896	1.0898	1.0897	1.0901	1.0897	1.0898	1.0901	1.0896	1.0896	1.0900	1.0898	1.0899
					Nonbonded Interatomic Distances[a]/Å							
OH···Se	2.7503	2.7672										
CH···O		3.1656		2.5776			2.6237					

[a] Calculated by the B3LYP/6-311+G** method. [b] C–H bond associated with intramolecular 1,5-CH···O interaction.

4.4.2 Molecular Geometries

The bond lengths and nonbonded interatomic distances for the 12 optimized conformers of MSE calculated by the B3LYP/6-311+G** method are given in Table 4.2. The O–H bond lengths for the GGg′ and G′Gg′ conformers are longer than those for other conformers by 0.004–0.005 Å. This lengthening of the O–H bond is obviously due to the formation of OH···Se hydrogen bonding. The OH···Se nonbonded interatomic distance in the GGg′ conformer is shorter than the corresponding distance in the G′Gg′ conformer. This implies that the hydrogen bonding in the GGg′ conformer is stronger than that in the G′Gg′ conformer, being consistent with the higher conformational stability of the GGg′ conformer.

The lengths of the C–H bonds associated with 1,5-CH···O interaction are shorter than the lengths of other C–H bonds by 0.003–0.004 Å. The mechanism of this bond shortening has been theoretically studied.[10-14] It was shown that the bond shortening originates from the redistribution of electron density in the C–H bond, induced when the bond comes close to a proton acceptor.[12] The geometry of the G′Gg′ conformer, in which 1,5-CH···O interaction and OH···Se hydrogen bonding are simultaneously involved, is peculiar in that the shortening of the relevant C–H bond is less prominent than that in the G′Gt and G′Gg conformers, and the CH···O nonbonded interatomic distance is much larger than that in the G′Gt and G′Gg conformers. These structural features of the G′Gg′ conformer indicate that the two interactions, 1,5-CH···O interaction and OH···Se hydrogen bonding, compete with each other, leading to diminished conformational stabilization by each of the interactions. It is noted, however, that the co-added effect of both interactions yet makes the G′Gg′ conformer considerably stable, being next to the most stable GGg′ conformer. A similar conformational property has also been observed for the G′Gg′ conformer of MTE.[8]

4.4.3 Matrix-Isolation Infrared Spectra and Molecular Conformation

The matrix-isolation infrared spectra in the 850–1500 cm⁻¹ region of MSE

annealed at different temperatures are shown in Figure 4.3, where the calculated spectra of the most stable three conformers, GGg′, G′Gg′, and GTg′, are also shown. The observed and calculated wavenumbers and the vibrational assignments for the GGg′ and G′Gg′ conformers are given in Tables 4.3 and 4.4. The wavenumbers calculated by density functional theory of B3LYP/6-311+G** were scaled by the WLS method,[22] which has been shown to give excellent agreement of the calculated wavenumbers with the experimental wavenumbers for a large number of organic and inorganic compounds.[23]

On annealing the matrix sample at 35 K, all of the observed bands become sharper, but their relative intensities do not change substantially. The well-defined bands at 920, 1069, 1072, 1162, 1256, and 1389 cm^{-1} are closely correlated to the normal vibrations of the GGg′ conformer. Although the calculated spectrum of the G′Gg′ conformer is similar in general to that of the GGg′ conformer, the observed bands at 924, 1065, 1157, and 1386 cm^{-1}, which are weaker than the corresponding bands for the GGg′ conformer, are unambiguously assigned to the G′Gg′ conformer. Most of the other bands observed in the matrix-isolated state are assigned to either or both of the GGg′ and G′Gg′ conformers (Figure 4.3). The weak bands at 985, 1044, and 1113 cm^{-1} are assigned, however, to neither GGg′ nor G′Gg′. These bands are well correlated to the vibrations of the GTg′ conformer with their calculated wavenumbers, 988, 1036, and 1120 cm^{-1}, respectively. These interpretations of the matrix-isolated spectra in the 850–1500 cm^{-1} region show that the GGg′ and G′Gg′ conformers are the dominant conformers in the matrix-isolated state. The GTg′ conformer also exists as one of the less populated conformers.

On heating the sample up to 41 K, the spectrum becomes broadened and new bands appear at 994, 1006, 1045, and 1198 cm^{-1}, etc. The broadened spectral feature is ascribed to the formation of aggregates of molecules resulting from the loosening of the matrix lattice in the heating process. The new bands are assigned to other conformers than GGg′ and G′Gg′.

The matrix-isolation infrared spectrum of MSE in the O–H stretching region shows two distinct bands at 3528 and 3538 cm^{-1} (Figure 4.4). These wavenumbers well correspond to the wavenumbers of O–H stretching vibrations
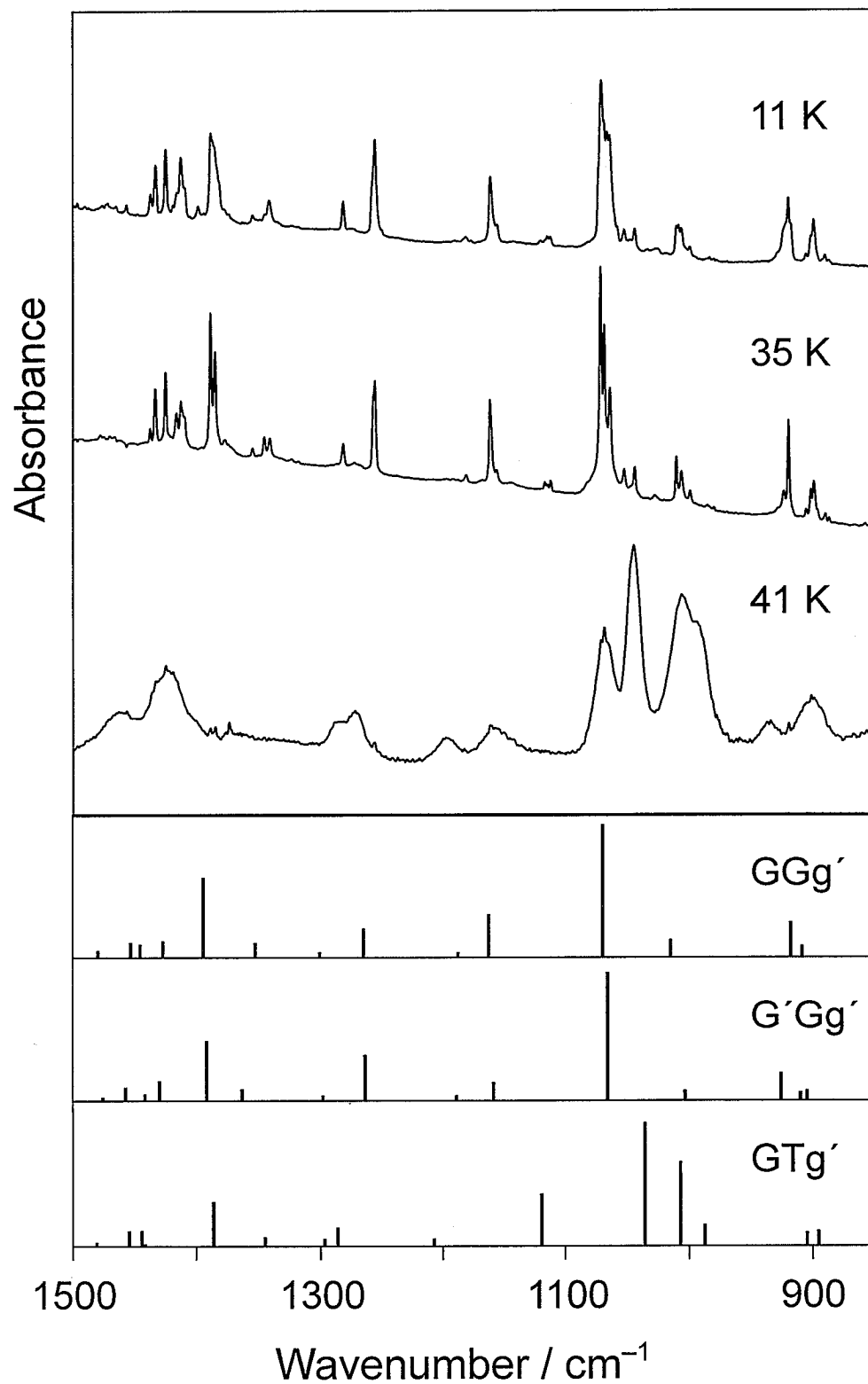
Figure 4.3 Infrared spectra in the 850–1500 cm^{-1} region of 2-(methylseleno)ethanol in an argon matrix annealed at 11, 35, and 41 K, and the calculated spectra of the GGg′, G′Gg′, and GTg′ conformers.

Table 4.3 Observed and Calculated Wavenumbers in the 850–3600 cm^{-1} Region[a] and Vibrational Assignments for the GGg′ Conformer of 2-(Methylseleno)ethanol

v_{obs}[b]/cm^{-1}	v_{calc}[c]/cm^{-1}	vibrational assignment[d]
3528 m	3549	O–H stretch (100)
	1481	C_bH_2 scissor (99)
1433 m	1454	CH_3 ip-asym deform (95)
1425 m	1446	CH_3 op-asym deform (92)
1413 w	1428	C_aH_2 scissor (92)
1389 m	1395	C_bH_2 wag (70), C–O–H bend (21)
1346 w, 1341w	1353	C_bH_2 twist (34), C–O–H bend (26), C_bH_2 wag (24)
1282 w	1301	CH_3 sym deform (100)
1256 m	1266	C_aH_2 wag (55), C_bH_2 twist (15), C–O–H bend (10)
1182 vw	1188	C_aH_2 twist (62), C_bH_2 rock (7)
1162 m	1163	C_bH_2 twist (42), C_aH_2 wag (31), C–O–H bend (30)
1072 s, 1069 s	1071	C–O stretch (74), C–C stretch (30), C–O–H bend (8)
1011 w, 1007 w	1016	C_bH_2 rock (34), C_aH_2 twist (20), C_aH_2 rock (15)
920 m	919	C_bH_2 rock (33), C–C stretch (32), C_aH_2 wag (7)
900 w	909	CH_3 ip-rock (46), CH_3 op-rock (37)
891 vw	906	CH_3 op-rock (57), CH_3 ip-rock (22), C–C stretch (7)

[a] Wavenumbers of the C–H stretching mode are omitted from the table. [b] Observed wavenumbers for an argon matrix. Approximate relative intensities: s, strong; m, medium; w, weak; vw, very weak. [c] Calculated by the B3LYP/6-311+G** method and scaled by the WLS method.[22] [d] Vibrational assignment for $CH_3SeC_aH_2C_bH_2OH$ is given in terms of the group coordinates. Key: sym, symmetric; asym, asymmetric; ip, in-plane; op, out-of-plane. Potential energy distributions (%) evaluated from the B3LYP/6-311+G** calculations are shown in parentheses.

Table 4.4 Observed and Calculated Wavenumbers in the 850–3600 cm^{-1} Region^a and Vibrational Assignments for the G′Gg′ Conformer of 2-(Methylseleno)ethanol

$\nu_{obs}{}^b$/cm^{-1}	$\nu_{calc}{}^c$/cm^{-1}	vibrational assignment^d
3538 w	3557	O–H stretch (100)
	1477	C$_b$H$_2$ scissor (100)
1437 w	1458	CH$_3$ ip-asym deform (95)
1425^e m	1443	CH$_3$ op-asym deform (93)
1417 w	1431	C$_a$H$_2$ scissor (90)
1386 m	1393	C$_b$H$_2$ wag (75), C–O–H bend (18)
1355 vw	1364	C$_b$H$_2$ twist (34), C–O–H bend (28), C$_b$H$_2$ wag (21)
1282^e w	1298	CH$_3$ sym deform (101)
1256^e m	1264	C$_a$H$_2$ wag (52), C$_b$H$_2$ twist (20), C–O–H bend (11)
1182^e vw	1189	C$_a$H$_2$ twist (56), C$_a$H$_2$ wag (12), C–C stretch (7)
1157 w	1159	C$_b$H$_2$ twist (39), C$_a$H$_2$ wag (29), C–O–H bend (24)
1065 m	1066	C–O stretch (71), C–C stretch (30), C–O–H bend (10)
1000 w	1004	C$_b$H$_2$ rock (32), C$_a$H$_2$ twist (23), C$_a$H$_2$ rock (15)
924 w	926	C$_b$H$_2$ rock (33), CH$_3$ ip-rock (24), C–C stretch (18)
903 w	910	CH$_3$ op-rock (94)
888 vw	905	CH$_3$ ip-rock (51), C–C stretch (24), C–O stretch (9)

^{a} Wavenumbers of the C–H stretching mode are omitted from the table. ^{b} Observed wavenumbers for an argon matrix. Approximate relative intensities: m, medium; w, weak; vw, very weak. ^{c} Calculated by the B3LYP/6-311+G** method and scaled by the WLS method.[22] ^{d} Vibrational assignment for CH$_3$SeC$_a$H$_2$C$_b$H$_2$OH is given in terms of the group coordinates. Key: sym, symmetric; asym, asymmetric; ip, in-plane; op, out-of-plane. Potential energy distributions (%) evaluated from the B3LYP/6-311+G** calculations are shown in parentheses. ^{e} Assigned also to the GGg′ conformer.
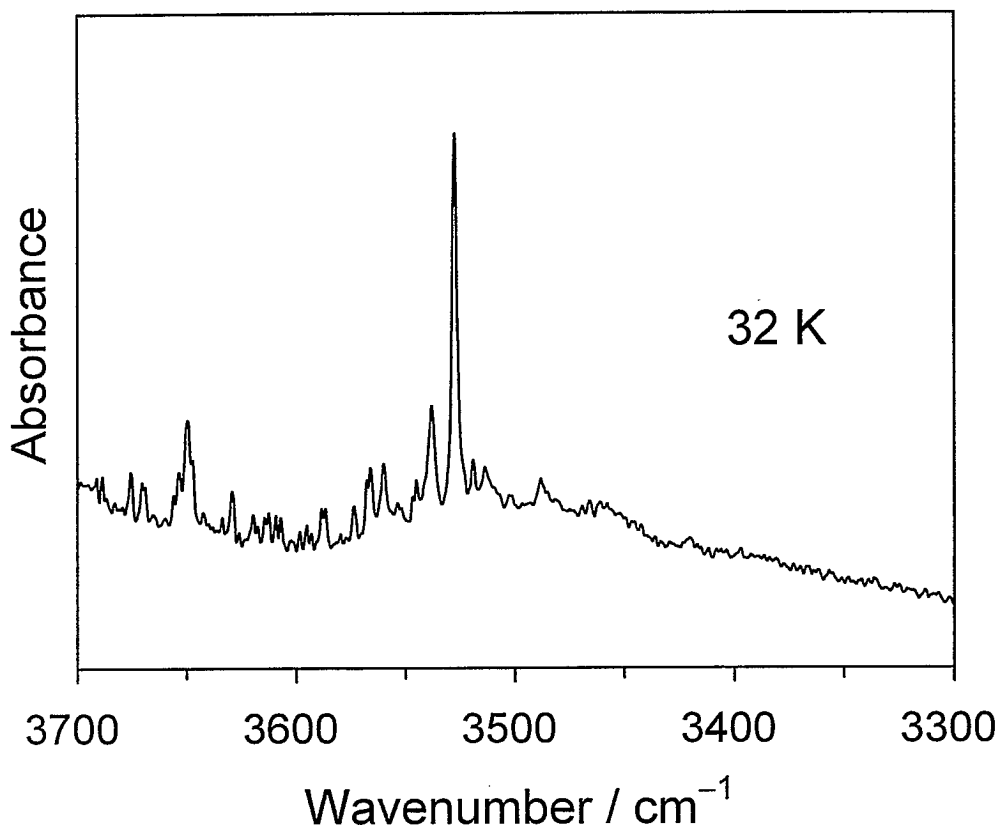
Figure 4.4 Infrared spectrum of 2-(methylseleno)ethanol in an argon matrix at 32 K in the O–H stretching region.

of intramolecular hydrogen bondings.[24] The normal coordinate calculations show that the bands at 3528 and 3538 cm^{-1} are correlated to the calculated wavenumbers 3549 cm^{-1} for the GGg′ conformer and 3557 cm^{-1} for the G′Gg′ conformer, respectively (Tables 4.3 and 4.4). The wavenumber difference between the two conformers is 10 cm^{-1} in the spectral observation and is 8 cm^{-1} in the calculation, supporting the present assignment of the bands. These results ensure that the conformers with intramolecular OH···Se hydrogen bonding, namely GGg′ and G′Gg′, exist in the matrix-isolated state. In addition to the two bands discussed above, an O–H stretching band is observed at 3649 cm^{-1}, which is assigned to free O–H stretching vibrations.[24] This spectral observation indicates the existence of conformer(s) without hydrogen bonding. The spectral features in the O–H stretching region are all consistent with the features in the 850–1500 cm^{-1} region with respect to the molecular conformation.

4.4.4 Raman Spectra in the Liquid and Solid States

The Raman spectra in the 400–850 cm^{-1} region of MSE in the liquid and solid states are shown in Figure 4.5. The observed and calculated wavenumbers and the vibrational assignments in this region are given in Table 4.5. Since the C–Se stretching wavenumbers are sensitive to the conformation,[25-28] the observed wavenumbers of MSE are examined in relation to the conformation around the $CH_3Se–CH_2–CH_2OH$ bonds. The C–Se stretching bands are observed at 568, 595, and 675 cm^{-1} in the liquid state, but the first band disappears on solidification. For methyl propyl selenide, $CH_3SeCH_2CH_2CH_3$, the bands observed in the liquid state at 559, 576, 646, and 660 cm^{-1} were assigned to the Se–CH$_2$ stretching mode of the GG, TG, GT, and TT conformations, respectively, around the $CH_3Se–CH_2–CH_2CH_3$ bonds and the band at 591 cm^{-1} was assigned to the CH$_3$–Se stretching mode.[26] In light of the previous assignments for methyl propyl selenide and of the results of the present normal coordinate analysis, the band at 568 cm^{-1} for MSE is assigned to the Se–CH$_2$ stretching mode of the GG and G′G conformations around the $CH_3Se–CH_2–CH_2OH$ bonds and the band at 675 cm^{-1} is assigned to the same mode of the GT and TT conformations. A band that can be assigned to the Se–CH$_2$ stretching mode of the TG conformation was not observed for MSE. The strong band at 595 cm^{-1} is assigned to the CH$_3$–Se stretching mode of all possible conformations.

In the liquid state, other conformation-sensitive bands are observed at 458, 740, and 795 cm^{-1}. The first band is assigned to the C–C–O bending mode of the GG and G′G conformations around the $CH_3Se–CH_2–CH_2OH$ bonds, the second band to the (Se)CH$_2$ rocking mode of the GT conformation, and the last to the (Se)CH$_2$ rocking mode of the GG, G′G, and TT conformations. On decreasing temperature, the relative intensities of the bands at 675 cm^{-1} (Se–CH$_2$ stretching) and 740 cm^{-1} ((Se)CH$_2$ rocking) increase, indicating that the GTx conformer is the most stable in the liquid state, where x denotes t, g, or g′. In the solid state, only the GTx conformer exists, as evidenced by the observation of the bands at 596, 677, and 738 cm^{-1} and missing of the other bands.

The above discussions show that the conformational stabilization of MSE in
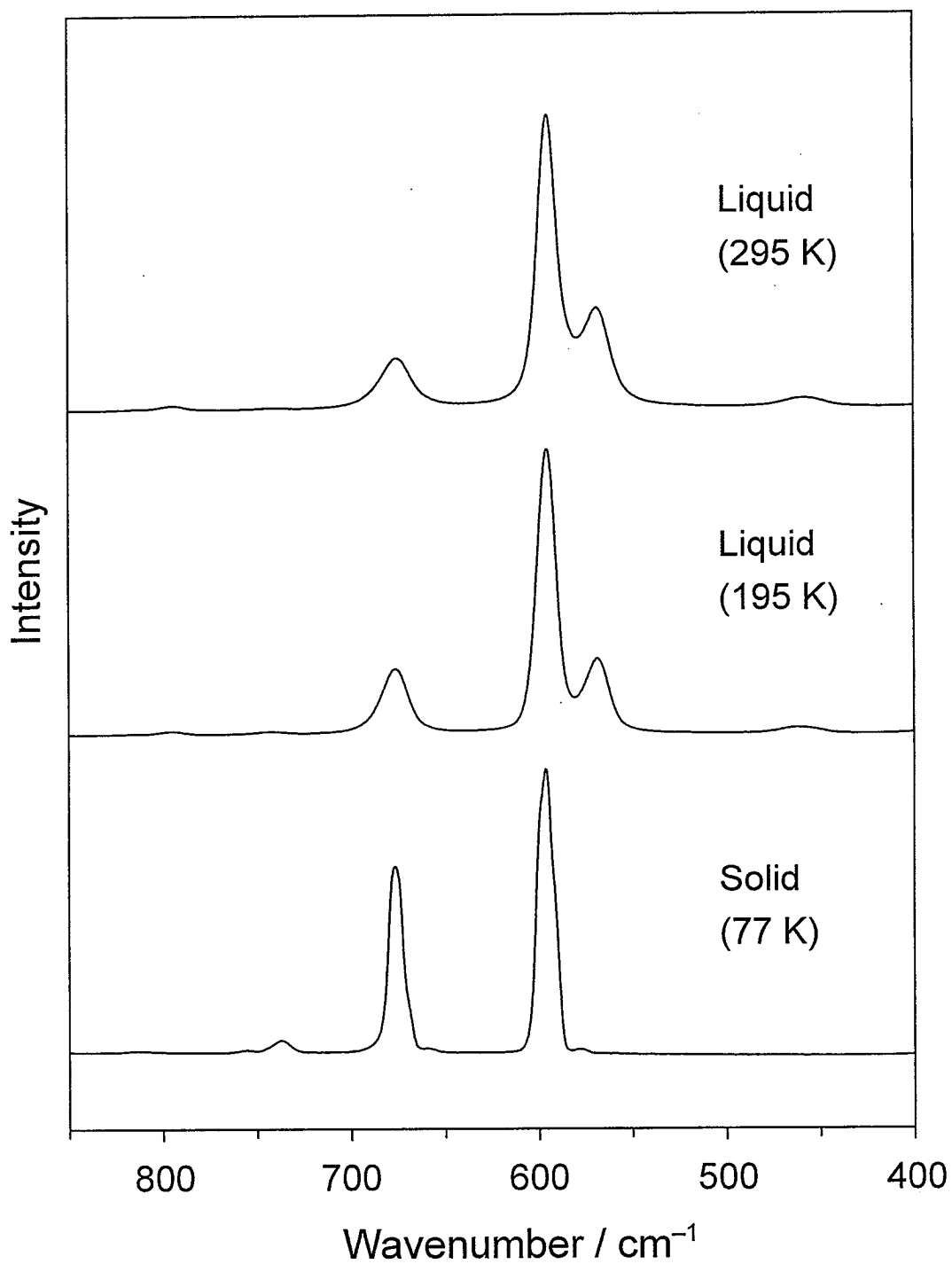
Figure 4.5 Raman spectra in the 400–850 cm^{-1} region of 2-(methylseleno)ethanol in the liquid state at 195 and 295 K and the solid state at 77 K.

Table 4.5   Observed and Calculated Wavenumbers in the 400–850 cm^{-1} Region and Vibrational Assignments for Conformers of 2-(Methylseleno)ethanol

v_{obs}^{a}/cm^{-1}		v_{calc}^{b}/cm^{-1}												vibrational assignment^{c}
liquid	solid	GGg'	G'Gg'	GTg'	G'Gt	GTg	GTt	G'Gg	TTg	TTt	TGt	TGg	GGt	
795 vw		801	796		794			794	775	784			795	C$_a$H$_2$ rock
740 vw	738 w			743		742	751							C$_a$H$_2$ rock
675 w	677 m			662		663	668		676	683				Se–CH$_2$ stretch
											584	588		Se–CH$_2$ stretch
595 s	596 s	579	578	577	579	577	578	579	580	582	574	577	579	CH$_3$–Se stretch
568 w		552	565		555			550					549	Se–CH$_2$ stretch
458 vw		469	469		437			450			441	452	444	C–C–O bend

^{a} Approximate relative intensities: s, strong; m, medium; w, weak; vw, very weak. ^{b} Calculated by the B3LYP/6-311+G** method and scaled by the WLS method.[22] ^{c} Vibrational assignment for CH$_3$SeC$_a$H$_2$C$_b$H$_2$OH is given in terms of the group coordinates.

the liquid and solid states is remarkably different from that in the matrix-isolated state. This difference implies that the effect of intramolecular OH···Se hydrogen bonding, along with 1,5-CH···O interaction, is a dominant factor in the conformational stabilization in the isolated state, while intermolecular interactions such as OH···O and OH···Se hydrogen bonding are more important than intramolecular interactions in the condensed phases.

4.4.5 Wavenumbers of Intramolecular Hydrogen-Bonded O–H Stretching Mode

The O–H stretching wavenumber has been considered as a measure of the strength of hydrogen bonding.[24,29] For discussing the stabilization energy by hydrogen bonding, the observed and calculated wavenumbers of the O–H stretching mode for MSE are compared with those for MTE and ME in Table 4.6, where the O–H bond lengths and O–H···X angles (X = Se, S, or O) are also given. The most stable conformers of MSE, MTE, and ME in the isolated state, namely GGg′, GGg′, and TGg′, respectively, are stabilized by intramolecular OH···X hydrogen bonding. The relevant data for non-hydrogen-bonded conformers, GGt, GGt, and TGt of MSE, MTE, and ME, respectively, are also given in Table 4.6. These conformers were chosen as the reference conformers by reason that they assume the same conformation around the $CH_3X–CH_2–CH_2OH$ bonds as the hydrogen-bonded conformers, but assume the trans conformation around the $CH_2–CH_2OH$ bond instead of gauche$^{\mp}$ in the hydrogen-bonded conformers.

The calculated results show that, for the conformers in which intramolecular OH···X hydrogen bonding is not involved, the O–H stretching wavenumbers and the O–H bond lengths are substantially the same for MSE (X = Se), MTE (X = S), and ME (X = O). For the conformers with intramolecular hydrogen bonding involved, on the other hand, the O–H stretching wavenumber of MSE is significantly lower than the wavenumber of ME and is only slightly lower than the wavenumber of MTE, although the stabilization energy by hydrogen bonding is almost the same for the three compounds as discussed in a preceding section. It is also noted that the lengthening of the O–H bond on the formation of

93

Table 4.6 Observed and Calculated O–H Stretching Wavenumbers, O–H Bond Lengths, and O–H⋯X Angles for 2-(Methylseleno)ethanol (MSE; X = Se), 2-(Methylthio)ethanol (MTE; X = S), and 2-Methoxyethanol (ME; X = O)

property	intramolecular hydrogen bonded			non-hydrogen bonded		
	MSE GGg′	MTE GGg′	ME TGg′	MSE GGt	MTE GGt	ME TGt
ν_{obs}/cm^{-1}	3528	3537	3625			
$\nu_{calc}{}^a$/cm^{-1}	3549	3556	3607	3648	3647	3651
O–H bond length^a/Å	0.9673	0.9669	0.9643	0.9610	0.9611	0.9607
O–H⋯X angle^a/deg	116.2	115.2	106.1			

^{a} Calculated by the B3LYP/6-311+G** method. Wavenumbers were scaled by the WLS method.[22]

hydrogen bonding in MSE and MTE is larger than in ME by about 0.003 Å. This geometrical property is consistent with the significantly lower wavenumbers of the hydrogen-bonded O–H stretching mode for MSE and MTE than for ME. It is shown, therefore, that the lowering of the O–H stretching wavenumbers for the hydrogen-bonded conformers of MSE and MTE is not immediately correlated to the stabilization energy by the relevant hydrogen bonding.

4.5   Conclusions

Implications of intramolecular interactions in the conformational stabilization of MSE have been studied by vibrational spectroscopy and density functional theory. The density functional calculations gave the conformational stabilization energy by intramolecular OH⋯Se hydrogen bonding as 14.5 kJ mol^{-1}, which is substantially the same as the corresponding energies for OH⋯O and OH⋯S hydrogen bonding.   The analysis of infrared spectra showed that the MSE molecules in an argon matrix assume primarily the GGg′ and G′Gg′ conformations with intramolecular OH⋯Se hydrogen bonding.   This spectral finding accords with the theoretically predicted stabilization energy by the hydrogen bonding.   The conformers of MTE and ME present in the matrix-isolated state are also stabilized by intramolecular OH⋯S and OH⋯O hydrogen bonding.   The theoretical results showed that intramolecular OH⋯Se hydrogen bonding is as strong as OH⋯O and OH⋯S hydrogen bonding.   In addition to intramolecular OH⋯Se hydrogen bonding, intramolecular CH⋯O attractive interaction plays an important role as a secondary interaction in the conformational stabilization of MSE. The stabilization energy by this interaction was estimated to be 5.6 kJ mol^{-1}.   The properties of OH⋯Se hydrogen bonding as revealed in this work should be important for elucidating conformational problems in molecular systems that contain selenium atoms.

References

(1)   Jeffrey, G. A.; Saenger, W. *Hydrogen Bonding in Biological Structures*; Springer: Berlin, 1994.

(2)   Yoshida, H.; Kaneko, I.; Matsuura, H.; Ogawa, Y.; Tasumi, M. *Chem. Phys. Lett.* **1992**, *196*, 601–606.

(3)   Tsuzuki, S.; Uchimaru, T.; Tanabe, K.; Hirano, T. *J. Phys. Chem.* **1993**, *97*, 1346–1350.

(4)   Jaffe, R. L.; Smith, G. D.; Yoon, D. Y. *J. Phys. Chem.* **1993**, *97*, 12745–12751.

(5)   Chapter 1 of this thesis.   Yoshida, H.; Harada, T.; Ohno, K.; Matsuura, H. *Chem. Commun.* **1997**, 2213–2214.

(6)   Ohno, K.; Tonegawa, A.; Yoshida, H.; Matsuura, H. *J. Mol. Struct.* **1997**, *435*, 219–228.

(7)   Yoshida, H.; Takikawa, K.; Ohno, K.; Matsuura, H. *J. Mol. Struct.* **1993**, *299*, 141–147.

(8)   Chapter 2 of this thesis.   Yoshida, H.; Harada, T.; Murase, T.; Ohno, K.; Matsuura, H. *J. Phys. Chem. A* **1997**, *101*, 1731–1737.

(9)   Chapter 3 of this thesis.   Yoshida, H.; Harada, T.; Matsuura, H. *J. Mol. Struct.* **1997**, *413/414*, 217–226.

(10)   Hobza, P.; Špirko, V.; Selzle, H. L.; Schlag, E. W. *J. Phys. Chem. A* **1998**, *102*, 2501–2504.

(11)   Hobza, P.; Špirko, V.; Havlas, Z.; Buchhold, K.; Reimann, B.; Barth, H.-D.; Brutschy, B. *Chem. Phys. Lett.* **1999**, *299*, 180–186.

(12)   Cubero, E.; Orozco, M.; Hobza, P.; Luque, F. J. *J. Phys. Chem. A* **1999**, *103*, 6394–6401.

(13)   Caminati, W.; Melandri, S.; Moreschini, P.; Favero, P. G. *Angew. Chem. Int. Ed.* **1999**, *38*, 2924–2925.

(14)   Gu, Y.; Kar, T.; Scheiner, S. *J. Am. Chem. Soc.* **1999**, *121*, 9411–9422.

(15)   Syper, L.; Mlochowski, J. *Synthesis* **1984**, 439–442.

(16)   Zhang, J.; Saito, S.; Takahashi, T.; Koizumi, T. *Heterocycles* **1997**, *45*, 575–586.

(17) Zhang, J.; Koizumi, T. *Synth. Commun.* **2000**, *30*, 979–986.

(18) Becke, A. D. *J. Chem. Phys.* **1993**, *98*, 5648–5652.

(19) Lee, C.; Yang, W.; Parr, R. G. *Phys. Rev. B* **1988**, *37*, 785–789.

(20) Frisch, M. J.; Trucks, G. W.; Schlegel, H. B.; Scuseria, G. E.; Robb, M. A.; Cheeseman, J. R.; Zakrzewski, V. G.; Montgomery, J. A., Jr.; Stratmann, R. E.; Burant, J. C.; Dapprich, S.; Millam, J. M.; Daniels, A. D.; Kudin, K. N.; Strain, M. C.; Farkas, O.; Tomasi, J.; Barone, V.; Cossi, M.; Cammi, R.; Mennucci, B.; Pomelli, C.; Adamo, C.; Clifford, S.; Ochterski, J.; Petersson, G. A.; Ayala, P. Y.; Cui, Q.; Morokuma, K.; Malick, D. K.; Rabuck, A. D.; Raghavachari, K.; Foresman, J. B.; Cioslowski, J.; Ortiz, J. V.; Stefanov, B. B.; Liu, G.; Liashenko, A.; Piskorz, P.; Komaromi, I.; Gomperts, R.; Martin, R. L.; Fox, D. J.; Keith, T.; Al-Laham, M. A.; Peng, C. Y.; Nanayakkara, A.; Gonzalez, C.; Challacombe, M.; Gill, P. M. W.; Johnson, B.; Chen, W.; Wong, M. W.; Andres, J. L.; Gonzalez, C.; Head-Gordon, M.; Replogle, E. S.; Pople, J. A. *Gaussian 98*, Revision A.5; Gaussian, Inc.: Pittsburgh, PA, 1998.

(21) Yoshida, H. *Molecular Modeling on Computers–A Guidebook of Molda*; Science House: Tokyo, 2000.

(22) Yoshida, H.; Ehara, A.; Matsuura, H. *Chem. Phys. Lett.* **2000**, *325*, 477–483.

(23) Matsuura, H.; Yoshida, H. In *Handbook of Vibrational Spectroscopy*; Chalmers, J. M., Griffiths, P. R., Eds.; Wiley: Chichester, 2001; Vol. 3.

(24) Hadži, D., Ed. *Hydrogen Bonding*; Pergamon: London, 1959.

(25) Ohno, K.; Hirokawa, T.; Aono, S.; Murata, H. *Chem. Lett.* **1976**, 1221–1224.

(26) Ohno, K.; Hirokawa, T.; Aono, S.; Murata, H. *Bull. Chem. Soc. Jpn.* **1977**, *50*, 305–306.

(27) Matsuura, H.; Ohno, K.; Murata, H. *Chem. Lett.* **1978**, 173–176.

(28) Ohno, K.; Mitsui, A.; Murata, H. *Bull. Chem. Soc. Jpn.* **1979**, *52*, 2178–2183.

(29) Scheiner, S. *Hydrogen Bonding: A Theoretical Perspective*; Oxford University Press: New York, 1997.

General Conclusions

In this thesis, the properties of intramolecular interactions, namely CH···O and CH···S interactions and OH···X (X = O, S, and Se) hydrogen bonding, have been presented. In particular, the conformational stabilization by intramolecular interactions has been described in detail. General conclusions drawn in the present work are summarized as follows.

For 1-methoxy-2-(methylthio)ethane (MMTE), $CH_3OCH_2CH_2SCH_3$, matrix-isolation infrared spectroscopy and density functional theory have clarified that the TGG′ conformer of MMTE has high conformational stability. Although the TGG′ conformer is the second most stable in an argon matrix, the energy difference from the most stable conformer TTG is only 0.69 kJ mol^{-1}. This result shows that 1,5-CH···O interaction plays an important role in the conformational stabilization of MMTE molecules. On the other hand, 1,5-CH···S interaction is not strong enough to stabilize the conformation of MMTE. With respect to the geometrical properties, the length of the C–H bond associated with 1,5-CH···O interaction is shorter than the lengths of other C–H bonds. These results manifest the important properties of intramolecular interactions, in which the C–H group is involved.

For a series of $CH_3XCH_2CH_2OH$ compounds [ME (X = O), MTE (X = S), and MSE (X = Se)], the matrix-isolation infrared spectra show that the conformers with intramolecular OH···X hydrogen bonding (X = O, S, and Se) primarily exist in an argon matrix. These experimental findings indicate that the most stable conformers of these compounds are stabilized predominantly by intramolecular hydrogen bonding. The density functional calculations show two remarkable characteristics of intramolecular hydrogen bonding. One is that the strength of the three types of intramolecular hydrogen bonding is almost the same. The other is that the wavenumber of hydrogen-bonded O–H stretching mode for MTE and MSE is considerably lower than the wavenumber for ME. These characteristics indicate that the lower shift of the hydrogen-bonded O–H stretching wavenumber is not immediately correlated to the strength of intramolecular hydrogen bonding.

For MTE and MSE, in addition to intramolecular OH···X hydrogen bonding, intramolecular CH···O interaction plays an important role as a secondary

interaction in the conformational stabilization.

A combination of matrix-isolation infrared spectroscopy and density functional theory is the most appropriate method for studying properties of intramolecular interactions and for making accurate conformational analysis of isolated molecules. The present studies should contribute significantly to further progress of structural chemistry, in particular, for understanding intramolecular interactions.